

2

ONR-URI Composites Program  
Technical Report No. 90-09

UIUC-NCCMR-90-09

**AD-A234 187**

STATIC AND CYCLIC COMPRESSIVE FATIGUE OF  
THERMOPLASTIC-MATRIX COMPOSITE IN  
AMBIENT AND MOISTURE ENVIRONMENTS

Kiet Van Chau\*\*

August, 1990

National Center for Composite Materials Research  
at University of Illinois, Urbana - Champaign  
A DoD University Research Initiatives Center funded by the  
Office of Naval Research, Arlington, VA

---

\*\* Graduate Assistant

91 3 27 093

## ABSTRACT

Advanced fiber-reinforced thermoplastic-matrix composites are being considered for many advanced engineering applications. Among various issues involved in these applications, deformation and failure behavior of the composites under static and cyclic compressive loading in ambient and moisture environments are of significant concern. In this study, a graphite-fiber/polyamide thermoplastic (AS4/J1) composite system is considered. Monotonic and cyclic fatigue compressive loadings are applied to the composite in ambient and moisture environments. The objectives of this research are to study: (1) compressive fatigue strength and failure modes; (2) compressive fatigue damage processes and associated property degradation; (3) effect of water absorption on compressive fatigue failure behavior; and (4) effect of lamination parameters on compressive fatigue properties. Test specimens were soaked in distilled water at 75°C until saturation. Five different laminates are studied, i.e.,  $[0]_{24}$ ,  $[0_2/90]_{4s}$ ,  $[0/90]_{6s}$ ,  $[90_2/0]_{4s}$  and  $[90]_{24}$ . Compressive specimens are designed to avoid Euler's structural buckling. In a unidirectional AS4/J1 composite, monotonic failure strength in compression along the longitudinal (i.e., 0°-fiber) direction is found to be much lower than that in tension, whereas the opposite is observed for the failure strength along the transverse (i.e., 90°-fiber) direction. Monotonic compressive stress-strain and cyclic stress vs. fatigue life relationships are obtained for all of the five laminates in both ambient and moisture environments. Compared with the specimens in an ambient environment, water-saturated specimens show an appreciably higher transverse strain to failure and lower transverse fatigue strength. However, not much difference between them is observed for longitudinal properties of the composite under static and cyclic loading.

DIST A PER TELECON MR. Y BARSOUM  
ONR/CODE 1132 SM  
4/1/91 CG

A-1

## 1. INTRODUCTION

Deformation and failure of advanced fiber composites subjected to monotonic and cyclic compression in ambient and moisture environments are subject areas of significant concern in recent developments and engineering applications of advanced materials [1-4]<sup>1</sup>. For example, testing of fiber composites under monotonic compression alone has been a controversial subject [5-7]. Specimen alignment, stress uniformity in the gage section and material compressive failure before specimen buckling are some of the major issues still unresolved in a proper uniaxial compressive test. In addition, moisture absorption of a polymer-matrix composite is known to cause plasticization of the matrix, leading to swelling of the composite, weakening of the fiber-matrix interface and local hygrothermally-induced stress in the material. Compression fatigue failure of polymer composites in a moisture environment is expected to have more complex failure modes, involving kinking, delamination, and other local cracking in "weak" areas of the composite, caused by non-uniform fiber dispersion, resin-rich localization, specimen-surface roughness, and stress concentrations due to imbedded defects and specimen geometry.

Compared with conventional thermoset-matrix composites, recently developed thermoplastic composites have the advantages of processibility, repairability, high temperature resistance, better interlaminar toughness, and superior damage tolerance [8-10]. These advantages have made thermoplastic composites attractive candidates for many advanced structural applications. Among various advanced engineering applications, the use of advanced thermoplastics composites in supersonic airframes and deep submersibles is under serious consideration. Clear understanding of mechanics and mechanisms of cyclic compressive fatigue failure

---

<sup>1</sup> Numbers in brackets refer to the List of References at the end of the thesis.

in ambient and moisture environments is essential to reliable design and analysis of composite structures.

While a large amount of literature are devoted to tensile fatigue of polymer composites, the study of compressive fatigue in a moisture environment has not been extensive. To the author's knowledge, no published work in the literature is available on the subject of compressive fatigue of thermoplastic-matrix composites in a moisture environment. This may be caused by difficulties involved in conducting accurate compressive fatigue experiments and complexities in evaluation of moisture diffusion in the composites.

The objectives of this study are to analyze: (1) compressive fatigue strength and failure modes; (2) compressive fatigue damage evolution and associated property degradation; (3) the effect of water absorption on compressive fatigue failure behavior; and (4) the effect of lamination parameters on compressive fatigue properties.

In the next section, a brief literature review is presented on monotonic and cyclic compressive loading on thermoplastic composites. Environmental effects on compressive material properties of the composites are also reviewed. In Sec. 3, an experimental study of a graphite fiber/polyamide thermoplastic composite under compressive loading is reported. Monotonic and cyclic compressive loadings are applied to the composite with five different laminate lay-ups in two environmental conditions. Composite compressive properties through the thickness of the laminate are also examined. An appreciable difference among them is observed. In Sec. 4, comparisons of experimental results obtained from different laminates in different testing environments are discussed. Important conclusions drawn from the research are given in Sec. 5.

## 2. LITERATURE REVIEW

In this chapter, a brief review of the literature is presented on the following topics: (a) compressive mechanical behavior of thermoplastic composites, (b) compressive fatigue of thermoplastic composites, (c) environmental effects on compressive mechanical behavior of thermoplastic composites.

Static and cyclic compressive behavior of polymer composites have long been a topic of interest to researchers. Significant research efforts have been directed at understanding the static failure behavior of the composites under compressive loading. Various compression test methods have been developed to evaluate the "true" compression failure strengths of the materials. Several failure theories and failure mechanisms are suggested. Recently, an extensive literature review on compressive deformation and failure of fiber composite materials has been conducted by Wang [11] and a review on compression of composite materials has been published by Camponeschi [12]. Past research efforts reported in these two documents have significant influence on compression research of thermoplastic composites in this study and the related ones below.

### 2.1 Mechanical Behavior of Thermoplastic Composites Under Compressive Loading

The compressive strength of a unidirectional carbon-fiber reinforced thermoplastic composite was evaluated by Lee and Trevett [13], using Celanese (ASTM D3410) and end-loaded fixtures. The results showed that the thermoplastic composite (APC2) has a compression strength similar to that of an epoxy composite in an ambient environment ( $\sim 1400$  MPa), but lower strength is found in the same epoxy composite at elevated temperatures than that of the thermoplastic composite. In addition, lower matrix shear modulus yields lower compressive strength of both

materials systems. The study reveals that thermoplastic composites and thermoset composites may have similar failure modes in compression, with a fracture path perpendicular to the applied load and oriented at a  $45^{\circ}$  angle to the thickness direction of the test specimen. Splitting and delamination were observed mostly in the specimen at a point one third of the distance along the gage length. Leeser and Leach [14] evaluated compressive properties of unidirectional and multidirectional laminate thermoplastic composites. Little correlation of compressive strength was found between an open-hole specimen and an after-impact specimen, both with the  $0^{\circ}$  fiber direction. The reason may be the difference in failure processes between the two specimens mentioned above. Longitudinal-fiber-direction compressive strength of a thermoplastic composite is found to be less than that of a thermoset composite.

PEEK prepreg tapes and fabric laminates under loading in unidirectional tension and compression were investigated by Scobbo and Nakajima [15]. SEM (scanning electron microscope) photos of the fracture surfaces under tension indicate that failure occurs primarily by fiber pull-out, or a combination of transverse (perpendicular to thickness) and shear deformation. The results indicate that compression modulus and strength depend on gage length and fiber waviness. Good adhesion between the matrix and fibers contributing to a higher strength in both the transverse tension and compression tests is observed. A model based on shear deformation is shown to predict a matrix-failure shear-strain for a  $\pm 45^{\circ}$  composite. The effect of delamination on compressive strength of carbon fiber/PEEK and carbon fiber/epoxy was investigated by Pavier and Chester [16]. A piece of 0.05 mm thick aluminum foil was placed between the ply during lay-up of the laminate for the initial delamination; different sizes of delamination were examined. Finite element analyses were performed to predict the failure loads. The

study shows that delaminations in a thermoplastic composite are less likely to grow prior to failure when comparing with those of a thermoset composite. The study also shows that an impact-damaged specimen results in a larger compressive strength reduction compared with the delamination-damaged specimen.

Guynn, Bradley and Elber [17-19] performed a detailed investigation on compressive failure of a thermoplastic composite laminate containing circular holes. C-scan, X-ray, SEM, and specimen sectioning examinations show that the damage zone is initiated by fiber microbuckling toward an unsupported surface. Compressive failure is proposed as initiation control in composites made of brittle resins and propagation control in composites made of ductile resin. Failure for a composite with a hole is initiated at the maximum stress concentration area, where kinking of a few fibers propagating across the specimen leads to catastrophic failure.

## 2.2 Fatigue of Thermoplastic Composites Under Compressive Loading

Over the years, many research projects have been conducted on fatigue damage of fiber thermoset composite. But there are only a few studies on fatigue damage of a thermoplastic matrix composite. In general, past experience on fatigue of thermoset composites are used as a guide for study of thermoplastic matrix composite. Black, Bakis and Stinchcomb [20,21] studied the fatigue damage of graphite/epoxy laminate composite with drilled center-holes under compression and tension-compression loading in the early 80's. The effort of this study was extended to tension-compression fatigue of a thermoplastic composite by Simonds, Bakis, Stinchcomb [22-24]. Through these series of year's study, the authors concluded that damage is initiated at the edge of the hole on all the composite specimens. For AS4/PEEK specimens, matrix cracks, delaminations, and fiber-fractures initiate

failure, with different stress levels resulting in different failure modes. At low cyclic stress level, the dominant growth direction is longitudinal and specimens fail in compression. At high cyclic stress level, the dominant damage growth direction is transverse and specimen fail in tension. Stiffness degradation is reported in both tension and compression moduli.

The frequency effect on fatigue of thermoplastic composite laminates was studied by Dan-Jumbo, Zhou and Sun [25]. Three different frequencies (0.4, 2, and 10 Hz) and two load levels (57.9% and 70% of the ultimate compressive load) with three types of laminates containing a center hole were studied. At lower frequency fatigue (0.4 Hz and 2 Hz), extensive delamination is observed, while at high frequency fatigue (10 Hz), global buckling seems to dominate the failure. The study also shows that the frequency effect on fatigue life of a thermoplastic composite depends greatly on the load level applied. At higher load level, frequency is proportional to the fatigue life. However, in general, fatigue life decreases as frequency is increased, especially above 2 Hz.

### 2.3 Environmental Effects on Mechanical Behavior of Thermoplastic Composites

Advanced composite materials can be susceptible to moisture. Extensive work on moisture absorption and moisture effects on mechanical behavior of a thermoset composite have been carried out by Springer and many others [26]. Recently, the introduction of thermoplastic composites revitalized the research efforts on the moisture effect on composite materials.

Cogswell and Hopprich [27] tested carbon fiber/PEEK in different solvents, aviation fluids, and in hot, wet environments. No significant effect on the mechanical properties of the tested samples was reported. At 70°C and moisture ageing to equilibrium, the carbon fiber/PEEK composite absorb 0.4% moisture by



weight. The wet and dry flexure strengths are identical at 120°C and 180°C. These strengths are 84% and 59%, respectively, of the strength at a room temperature. Lhymn and Schultz [28] precondition a short fiber-reinforced thermoplastic composite in water to test its toughness. The study shows that in a water environment, bonding of the carbon-fiber/PPS matrix interface is relatively poor compared with the PPS/glass fiber interface. Cracks in the specimen are formed slowly but propagate fast, which reveal a micro-crazing appearance. Kays and Hunter [29] conduct tension tests on thermoplastic composite to determine the mechanical property in room environment and after exposure to humidity and solvents. A 10% to 25% reduction in tensile strength is reported for moisture saturated fiber glass fabric/thermoplastic composites. Valentin, Paray and Guetta [30] examine short and continuous fiber/thermoplastic composites at three different temperatures and relative humidity levels. Water absorption in the Pa66 matrix composite is found to obey the Fickian diffusion law at temperatures below or equal to 70°C. However, higher temperatures, thermal ageing, oxidation, and leaching can disturb the diffusion behavior. Three-point bending tests are performed on dry and saturated composites. The main consequence of the water uptake is plasticization of the matrix, which leads to a drop in mechanical properties. Hoa, Lin and Chen [31] study the effects of moisture absorption on the mechanical behavior of glass-reinforced polyphenylene sulfide (PPS) composite. Moisture absorption of 25% by weight is reported. Large areas of voids and crevices are suggested as the paths for water to penetrate. Debonding between glass fibers and PPS matrix is observed. The degree of crystallinity is also an important factor affecting the results of the 25%-46% and up to a maximum of 60% tensile strength reduction. Wang and Springer [32] conduct experiments on PEEK 150P polymer and APC-2 composite exposed to humid air. Effects of moisture content and crystallinity on fracture toughness are

evaluated. From the scattered results and the test conditions, the report concludes that fracture toughness is not affected by the crystallinity or the moisture content of the material.

### 3. EXPERIMENTAL PROGRAM

#### 3.1 Material

The thermoplastic composite material used in this study was provided by E.I. duPont de Nemours and Company, Inc. The composite was a continuous-fiber reinforced thermoplastic system, with a nominal fiber volume fraction of 60%. The fibers were commonly used AS4 graphite fibers. The matrix was a thermoplastic polyamide resin, also called J1 polymer. Unidirectional composite laminae were melt-impregnated 0.005-inch thick AS4/J1 preregs. The molding procedure for a 24-ply composite lay-up was as follows: mold preheated at 300°C and 70 psi, composite consolidated at 300°C and 1000 psi, air cooled for 2 hours at 50°C and 1000 psi. Composite laminate plates of a 12x12 inch dimension with  $[0]_{24}$ ,  $[90]_{24}$ ,  $[0_2/90]_{4s}$ ,  $[0/90]_{6s}$  and  $[90_2/0]_{4s}$  layups were prepared for the experiments [33,34].

#### 3.2. Specimen Design and Analysis

Dimensions and geometric configurations of compressive test specimens with different lay-ups are given in Table 1 and Fig. 1. The specimen design was conducted by taking consideration of the end loading effect, structural buckling, the grip end effect and stress uniformity in the gage section.

##### 3.2.1 End Loading Effect and Stress Uniformity

The Saint-Venant decay length was calculated first. A finite element analysis (Fig. 2) was performed to determine the optimal specimen geometry. Stress uniformity was ensured in the gage section under applied compressive loading. The characteristic decay length  $\lambda$  can be approximated by [35] :

$$\lambda \sim \frac{b}{2\pi} \left( \frac{E_1}{G_{12}} \right)^{\frac{1}{2}},$$

where subscripts 1 and 2 refer to the loading direction and the transverse direction. The  $\lambda$  is an axial distance over which the stress decays to within 1% of the uniform nominal level, and  $b$  is the maximum cross-sectional dimension,  $E_1$  is the axial Young's modulus, and  $G_{12}$  is the interlaminar shear modulus.

### 3.2.2 Structural Buckling

The buckling load of a composite specimen was estimated first to ensure that, in the static and cyclic compressive experiments, compressive material failure precedes structural instability. The specimen gage length was shortened to avoid any structural buckling before the composite compressive strength was reached. Estimation of the Euler buckling stress was based on the following relationship given in [36]:

$$\sigma_b = \frac{E_1}{\frac{12}{\pi^2} \left( \frac{L_0}{t} \right)^2 + 1.2 \left( \frac{E_1}{G_{12}} \right)},$$

where  $L_0$  is the specimen gage length and  $t$  is the thickness of the specimen.

### 3.2.3 End Gripping Effect

The specimens shown in Fig. 1 and Table 1 all had the same width in the gripping section. These were designed to fit the specimen housing of the hydraulic

grip wedges. The one-inch gripping length was introduced to provide enough end support to ensure geometric stability when the compressive loading was applied. The curvature of the specimen shoulder was designed to ensure an approximate uniform stress state in the gage section to avoid failure at grip ends. However, the shoulder radii also introduced a stress concentration in the shoulder section of the specimen. Finite element analyses with 8 noded quadrilateral elements were used to minimize stress concentrations in the specimen. All of the analyses were performed on the Convex C1-XP computer. Constant stress contour plots for a  $[0]_{24}$  AS4/J1 composite under a controlled-loading are shown in Fig. 2. Stress concentrations were highest for the  $[0]_{24}$  specimen in the end-shoulder area. The specimen which had the lowest stress concentration was the  $[90]_{24}$  composite.

### 3.3 Moisture Conditioning of Composite Specimens

#### 3.3.1 Ambient Environment

Specimens were machined from composite plates provided by DuPont. All of the specimens were kept in plastic bags in deccators until testing. The high-cycle fatigue test experienced a slight drop of night-time temperature, but this did not affect the experimental results in general.

#### 3.3.2. Moisture environment

Specimens tested in a wet environment were preconditioned at 75°C in small jars containing distilled water for eight months. Specimens were taken out periodically to weigh on a high-precision Mettler H78AR analytic balance. Accuracy of the weight gain was within a range of 0.0001 g. The weight change as a function of time was recorded. Moisture absorption of approximately one-percent weight gain for the composite was reported at the water saturation level.

Moisture content of the composite during absorption is represented by

$$M = G (M_{\max} - M_0) + M_0,$$

where  $M_0$  is the initial moisture content of the composite in an ambient environment,  $M_{\max}$  is the moisture content of the composite after water saturation, and  $G$  is a time dependent parameter. The value of  $G$  is given as [37,38]

$$G = 1 - \frac{8}{\pi^2} \sum_{j=0}^{\infty} \frac{\exp \left[ -(2j+1)^2 \pi^2 \left( \frac{D_x t}{h^2} \right) \right]}{(2j+1)^2},$$

where  $D_x$  is the diffusivity of the composite in the direction normal to the surface,  $t$  is time and  $h$  is the thickness of the composite.

Moisture conditioning during a fatigue test was satisfied by attaching a small amount of absorbent cotton around the gage section in the specimen. A section of rubber tube was used to hold the cotton in place. The cotton was moistened with distilled water by dripping the water periodically from a syringe with a long needle.

### 3.4. Static Strength and Cyclic Fatigue Test Procedure and Data Acquisition

#### 3.4.1. Static Compression

Experiments were performed on an Instron 1331 servohydraulic test system with a 20-kip load cell. A pair of hydraulic grips was initially aligned with a straight steel bar with strain gages mounted on both sides of the bar. Compressive end loading applied to the specimen was introduced by the piston inside the grips. No end tab was used on the specimen. Brass shims were applied for specimens with a

thickness smaller than that of the original design. Edges of the grip wedges were smoothed down with a metal file to prevent local biting into the specimen.

An 80286 Dell personal computer was used for test control and data acquisition. All of the test data were stored in the computer memory for further analysis. Strain measurements were obtained by a highly sensitive MTS 632 extensometer, attached on the surface of the specimen. Knife edges of the extensometer were fixed to specimen surfaces by elastic rubber bands. The moduli or stiffnesses of a composite laminate were obtained by measuring the initial slope of the stress-strain curve on an X-Y plotter. A stroke-control mode was used for the monotonic compression test with the cross head moving at a speed of  $2.9 \times 10^{-5}$  in/sec.

A wet monotonic compression test was performed right after a specimen was taken out of the environmental chamber. A coating of Vaseline gel was applied to the specimen to prevent moisture evaporation.

#### 3.4.2 Cyclic Compressive Fatigue

Cyclic compression-compression fatigue experiments were conducted to determine the stress-life relationship, the composite fatigue limit, and failure criteria. Multiple tests at each stress level were usually conducted to ensure the consistency of the results. Those surviving  $10^6$  cycles were considered as fatigue runouts. Cyclic fatigue tests were performed at a load-control mode with a minimum to maximum fatigue stress ratio of 10 ( $R=10$ ). A sine-wave loading function was used and fatigue frequencies were 1 Hz to 10 Hz. Most of the specimens run at 10 Hz were subjected to the stress at the fatigue limit level, which usually took up to  $10^6$  cycles. Both the loading function and the frequency were set by a controls on the function generator. Wet compression-compression fatigue experiments were performed by

wrapping with water absorbent cotton in the gage section. Water was injected periodically to ensure the specimen was in a saturated moisture environment.

### 3.4.3 Specimen Curing Effect

The curing effect on the thermoplastic composites was evaluated by slicing the thick section composite laminate. An uniaxial thick composite laminate with a 0.6 inch thickness was sliced with a diamond saw blade into three different (0.13 inch) specimens at different locations through the thickness. Symmetry of the laminate was taken into account. The center section was sliced to be one "center" specimen, 0.005" from each side of the "center" specimen was sliced and gave two "middle" specimens. On another piece of thick-composite coupon, from each face of the laminate was sliced to give two "end" specimens, a "center" specimen was also sliced at the center of the coupon. Monotonic compression and cyclic compression-compression fatigue experiments were performed for uniaxial and transverse direction composites at room temperature.



## 4. RESULTS AND DISCUSSION

### 4.1 Compressive Behavior under Monotonic Loading

Failure strengths and elastic stiffnesses of the AS4/J1 thermoplastic composite laminates under monotonic compression were obtained and shown in Table 1. In conducting uniaxial monotonic compression experiments, two important factors were considered: suitable test fixtures and proper specimen design. From experimental observations, the aforementioned self-aligned hydraulic grips and dumbbell-shape specimens used did not show a failure mode in bending or buckling. Thus, good specimen alignment was assumed. With this type of specimen design, stress concentrations were expected to have a uniform stress distribution in the gage section and at the ends of each shoulder. The constant stress contour plots (Figs. 2) from an FEM analysis confirmed these. Most of the specimens failed at the border of the gage section and the end of the shoulder, where axial compressive stress was the highest. To determine the validity of the tests with the present specimen design and the gripping system, the results were compared with those obtained by the recommended standard ASTM compression test method, using the well-known ITTRI compression test fixture. The results in Table 3 have shown that the compressive strengths obtained in the tests with the ITTRI fixtures have values of 7% to 12% higher than those obtained in the present experiments. In general, test results from the composite specimens in hydraulic grips yielded slightly lower strengths. The variations were expected as a large amount of data scatter from both test methods was observed. Exact failure modes in the compression test specimens were difficult to observe because fracture surfaces were smashed together after the initial failure. In all of the specimens with the five different laminate lay-ups that were

tested, in-plane shear seemed to initiate the general compressive failure in the composite.

For the unidirectional  $[0]_{24}$  laminate specimens, the compressive strength of the composite was found to be fiber-dominant. The composite laminate yielded a high compressive strength of 110 ksi at 0.6% failure strain (Fig. 4). In the  $[90]_{24}$  composite specimens, structural buckling was observed from time to time because of the low axial stiffness of the composite laminate. The gage length of the  $[90]_{24}$  composite specimen was not able to be reduced further owing to the minimum size requirement of the extensometer placed on the surfaces of the specimen for strain measurements. In most of the  $[90]_{24}$  composite specimens, in-plane shear flow was observed to occur at the compressive failure within the gage section. Local stress concentrations did not seem to have much effect in this laminate specimen, because of the large shoulder radius and the small  $W/w$  value. Significantly nonlinear compressive stress-strain relationship with a 4% compressive failure strain was observed (Fig. 5).

For the composite specimens with the cross-ply lay-ups,  $[0_2/90]_{4s}$ ,  $[0/90]_{4s}$ , and  $[90_2/0]_{4s}$ , delaminations were generally observed after specimen failure. The post-failure delaminations were caused by interlaminar stresses developed due to large out-of-plane deformations during post-buckling. Delaminations were mostly observed at the ply interfaces not too far from the failure surface, suggesting that compressive failure initiated by delamination was not likely. In general, compressive stiffnesses, compressive strengths, and stress-strain relationships of these composites were found to be proportional to the number of  $0^\circ$  and  $90^\circ$  laminae in the laminates (Fig. 6-8). The failure also appeared to be in an in-plane shear mode, but the presence of longitudinal fibers seemed to blunt the cracks appeared in the

90° laminae. Failure in all of these specimens was developed abruptly without any nonlinear flow.

The compressive strengths and stiffnesses of the AS4/J1 thermoplastic composite laminates in an ambient environment exhibited rather large scatter. The higher the strength, the larger the scatter. The strength variation can be as high as 20 ksi for the  $[0]_{24}$  composite laminates and 5 ksi for the  $[90]_{24}$  laminates. The compressive property variations may be caused by fiber misalignment, local residual stress concentrations between laminae, and such defects as microvoids or initial laminate curvatures.

#### 4.2 Compressive Stress-Fatigue Life Relationship

Cyclic compression experiments were performed on the same test system as for the aforementioned monotonic compression experiments. We note that the hydraulic grip system was chosen in the compressive fatigue experiments because it provides proper gripping for the specimen under cyclic dynamic loading over an extended period of time. The standard IITRI compressive test fixtures were not applicable in this experiment due to the following reasons. The IITRI test fixture were originally design for monotonic static compression test only. The bottom half of the IITRI grip housing was not fixed to the actuator rod and would vibrate out of position under dynamic cyclic fatigue loading. The guiding rods on the grip housing, which were to keep the alignment of the specimen during the test, would introduce large friction under cyclic loading. Also the mechanical locking system between the grip and the specimen would not be sustained over repeated loading.

Compressive fatigue tests were performed at different stress levels for the aforementioned composite laminate systems. The stress levels were applied by gradually stepping down from the ultimate compressive strengths of the composites.

The stress level where the specimens survived at fatigue cycles exceeding  $10^6$  cycles was considered to be the fatigue limit. Cyclic compressive stress-fatigue life relationships of the composite laminates studied are shown in Figs. 9-13. It appears that the cyclic compressive stress vs. fatigue life relationships of the laminates are well behaved. Scattering of the fatigue failure data at different stress levels was relatively small. The compressive fatigue experiment under a low cyclic stress had higher cycles to failure ( $N_f \cong 10^5$  or  $10^6$ ); a frequency of 8 Hz to 10 Hz was applied to reduce the experiment time. The flat slope of the compressive S- $N_f$  data for the composite laminates with several lay-ups suggested that these composite laminate systems were not fatigue sensitive. The fatigue limit of the  $[0]_{24}$  composite was at about 70% level of the ultimate compressive strength. For the  $[90]_{24}$  composite, the compressive fatigue limit was approximately 60% of the ultimate compressive strength. For the  $[0_2/90]_{4s}$  laminates, it was 80%. For  $[0/90]_{6s}$ , it was 80%, and for  $[90_2/0]_{6s}$ , it was 78%.

Failure modes of the composite laminates under compressive fatigue appeared to be similar to those under monotonic compression. In-plane shear failure of the specimens was generally observed. Compared with the specimens under monotonic compression, post fatigue failure modes showed a larger amount of delamination in the cross-ply laminates. However, no obvious delamination was observed before specimen failure. Only outermost ply delaminations were observed occasionally during the high-cycle fatigue. Specimen buckling was not observed in the fatigue failure because of the low stress applied relative to buckling strengths of the specimens. No sign of fatigue failure initiated by fiber buckling in the composite under cyclic compression was observed.

#### 4.3 Stiffness Degradation During Compressive Fatigue

Cyclic compressive loading was applied at the 55% and 60% levels of ultimate compressive strengths of the  $[0]_{24}$  and  $[0_2/90]_{4s}$  composite laminates. Elastic stiffnesses along the loading direction were evaluated periodically to examine damage development and associated stiffness degradation. Elastic stiffnesses of both composite laminates change slightly throughout the fatigue cycles as shown in Fig. 14 and 15. A slight increase in axial stiffness of the  $[0]_{24}$  composite were observed, whereas slight decrease in stiffness were found in the  $[0_2/90]_{4s}$  laminate. Monotonic compression tests were performed on the specimens after  $10^6$  cycles to evaluate the residual stiffnesses of the material. Stress-strain curves of the fatigued specimens are compared with those of the virgin composites in ambient and moisture-saturated environments in Figs. 16 and 17. The results do show appreciable changes between the composite specimens tested. Thus these fiber-dominated thermoplastic composites are fatigue sensitive. Furthermore, failure modes in these composite systems were observed to be mainly caused by initiation followed by catastrophic fracture.

#### 4.4 Processing Effect on Monotonic and Fatigue Compressive Behavior

The effect of processing may be manifested by property gradients through the laminate thickness. To examine the processing effect on static and cyclic compressive fatigue behavior of the thermoplastic composite, a 108-ply unidirectional thick composite laminate specimen was sliced at three different thickness levels. Specimens obtained from the three locations were named as "center", "middle", and "surface" section specimens. A small overlap occurred through the thickness of the middle-section specimens and the surface section specimens. Symmetry was assumed for specimens derived from the material away from the mid-plane of the laminate. Monotonic and compressive-compressive

fatigue experiments were performed on a series of these specimens with longitudinal and transverse fiber orientations. Mechanical properties of these specimens are shown in Table 4. From the results, these sectioned specimens were observed to have consistent values of failure strengths (Figs. 18, and 19).

Large compressive strains under loading were most obvious in the sectioned- $90^\circ$  specimens obtained from the center portion of the thick composite. A failure strain up to 9% was observed, as compared with the 3% failure strain for the sectioned surface specimens (Fig. 19). Compressive constitutive properties at different locations through the thickness of the  $[0^\circ]_{108}$  specimen did not show an obvious difference, because of the fiber dominant nature. The reason for the large compressive failure strain of the center-section  $90^\circ$  composite specimen may be related to the processing of the composite and the matrix-dominated compressive failure. (When the thick composite plate was air-cooled from molding, outer layers and inner layers may be cooled at different rates, leading to different matrix and interface morphology with differential material properties in the thick composite.)

Compressive fatigue behavior of all three sectioned specimens did not show much difference; this is true for both longitudinal and transverse specimens (Figs. 20, and 21). Comparing the compressive  $S-N_f$  results for the sectioned specimens with those from the 24-ply corresponding materials, the only difference observed was the fatigue limit. The fatigue limit of the center-sectioned specimen was higher than that of the surface-sectioned specimen. This appeared true for both  $0^\circ$  and  $90^\circ$  cases. Scattering of fatigue data of the sectioned composite specimen was smaller than those of the 24-ply laminate specimens. Failure modes in the sectioned specimen and in the thin 24-ply specimens were similar for both  $0^\circ$  and  $90^\circ$  cases. The in-plane shear mode failure was observed under both monotonic and fatigue loading. Global structural buckling was not observed when the sectioned  $90^\circ$

specimen was tested under monotonic compression. This was due to the uniform thickness and flatness when the composite was sliced from the thick laminate. However, the 24-ply composite usually had a slight curvature due to processing, leading to possible specimen premature buckling before the final compressive failure. From all of the observations, it seemed the thick-section composite had a larger strain to fracture and a slightly higher compressive strength.

#### 4.5 Effect of Moisture on Compressive Monotonic and Cyclic Fatigue Behavior

Composite specimens were soaked in distilled water for extended periods of time (approximate 8 month). Moisture saturation in the specimens was reached at the time when no additional weight gain was observed for a period of time. Plotting the percentage of weight gain in the specimen versus the square root of time exposed, we observed the AS4/J1 composite followed Fickian's diffusion law, as shown in Figs. 22 and 23. A detail study of moisture transport in the composite material system was performed in a separate study [39]. Comparing the stress-strain curves of the composite specimens in the ambient and moisture environments, we observed that the amount of material nonlinearity is aggravated in the water-saturated environment (Figs. 4-8). The increase in nonlinearity was most obvious for the composite with a 90°-ply lay-up owing to the matrix-dominated nature. A slightly lower ultimate compressive strength was observed for the water-saturated specimen than that of the dry specimen.

The ultimate static compressive strength and the cyclic compressive fatigue strength of water-saturated specimens were found to be more consistent when compared with the specimens in the ambient environment (Figs. 9-13). The compressive  $S-N_f$  curve of the  $[90]_{24}$  composite in a water-saturated environment was no longer a straight line. The fatigue limit of the 90°-ply composite in the

specimen was tested under monotonic compression. This was due to the uniform thickness and flatness when the composite was sliced from the thick laminate. However, the 24-ply composite usually had a slight curvature due to processing, leading to possible specimen premature buckling before the final compressive failure. From all of the observations, it seemed the thick-section composite had a larger strain to fracture and a slightly higher compressive strength.

#### 4.5 Effect of Moisture on Compressive Monotonic and Cyclic Fatigue Behavior

Composite specimens were soaked in distilled water for extended periods of time (approximate 8 month). Moisture saturation in the specimens was reached at the time when no additional weight gain was observed for a period of time. Plotting the percentage of weight gain in the specimen versus the square root of time exposed, we observed the AS4/J1 composite followed Fickian's diffusion law, as shown in Figs. 22 and 23. A detail study of moisture transport in the composite material system was performed in a separate study [39]. Comparing the stress-strain curves of the composite specimens in the ambient and moisture environments, we observed that the amount of material nonlinearity is aggravated in the water-saturated environment (Figs. 4-8). The increase in nonlinearity was most obvious for the composite with a 90°-ply lay-up owing to the matrix-dominated nature. A slightly lower ultimate compressive strength was observed for the water-saturated specimen than that of the dry specimen.

The ultimate static compressive strength and the cyclic compressive fatigue strength of water-saturated specimens were found to be more consistent when compared with the specimens in the ambient environment (Figs. 9-13). The compressive S-N<sub>f</sub> curve of the [90]<sub>24</sub> composite in a water-saturated environment was no longer a straight line. The fatigue limit of the 90°-ply composite in the



moisture-saturated environment was significantly lower than that in the ambient environment. However, no obvious difference in fatigue limit of the  $0^0$ -ply-dominant composite was observed in an ambient and a moisture-saturated environment. From the experimental results, we concluded that moisture absorbed in the composite had similar characteristics to a common plasticizer in the matrix. The absorbed water molecules acted as a relaxing agent to reduce initial residual stress in the material. The moisture also softened the polymer matrix and reduced the strength of the composite, especially in a cyclic compressive fatigue situation. Fiber-matrix interface debonding caused by moisture penetration did not seem to appear. Failure modes in the water-saturated specimens were much the same as those in the dry specimens. The in-plane shear failure with post delaminations were also observed in the moisture-saturated composite laminates. The failure in the specimen was also noted to initiate along the edge of the gage section and at the shoulder end. *Post-failure delaminations* in the water-saturated specimens were observed to be not as severe as those observed in the specimens tested in an ambient environment.

## 5. CONCLUSIONS

Monotonic and cyclic compressive fatigue of a thermoplastic-matrix composite have been studied. Experiments were conducted on AS4/J1 composite laminates with  $[0]_{24}$ ,  $[0_2/90]_{4s}$ ,  $[0/90]_{6s}$ ,  $[90_2/0]_{4s}$  and  $[90]_{24}$  layups. A study of the influence of water absorption of the composite on both static and cyclic compressive fatigue of the composite laminates was conducted. Through-the-thickness property variation in a thick-section (108-ply) AS4/J1 composite was also examined under monotonic and cyclic compressive fatigue loading.

Results from experiments on as-received and water-saturated AS4/J1 composite laminates lead to the following conclusions:

1. Compressive failure under both monotonic loading and cyclic fatigue in both ambient and moisture environments is observed to be initiated at stress concentration areas followed by a catastrophic fracture.
2. Significant non-linearity of the compressive stress-strain relationship is found in the  $90^\circ$  AS4/J1 thermoplastic composite.
3. Moisture diffusion in the composite under  $75^\circ\text{C}$  over a 8 month period in a distilled water environment follows the classical Fickian law of diffusion.
4. Cyclic compressive stress-fatigue life relationships of the AS4/J1 composite laminates with various layups in an ambient environment follow an approximate linear behavior.
5. Water saturation in the thermoplastic composites affects severely the compressive stress-fatigue life relationships of the  $90^\circ$  AS4/J1 composite and the  $90^\circ$ -ply dominated composite laminates. The compressive stress-fatigue life relationships of the water saturated composite laminates are no longer linear.

6. Scattering of compressive failure strength of the thermoplastic composite under monotonic compressive and cyclic compressive fatigue was largely reduced in the composites with water saturation.

7. Compressive stiffnesses of  $[0]_{24}$  and  $[0_2/90]_{24}$  AS4/J1 composites during cyclic fatigue in an ambient environment remain relative constant till catastrophic compressive fracture.

8. The static compressive stress-strain relationship of a center-sectioned composite specimen has a higher nonlinearity, as compared with that of a surface-sectioned specimen. This nonlinearity is aggravated greatly in the transverse  $90^\circ$  fiber composite. The detail study of compressive properties through the thickness of a thick composite gives a good understanding of the processing effect on compressive material properties of the composite.

9. Cyclic compressive stress-fatigue life relationships of the sectioned specimens do show a difference in compressive properties through the thickness of the composite. Processing effects on the AS4/J1 compressive fatigue properties should be noted in the design of thermoplastic composite structures.

TABLE - 1  
 DIMENSIONS OF COMPRESSIVE TEST SPECIMENS  
 WITH DIFFERENT LAMINATE LAY-UPS

| <u>Layup (<math>\theta</math>)</u> | <u>L (in.)</u> | <u>L<sub>0</sub> (in.)</u> | <u>R (in.)</u> | <u>w (in.)</u> | <u>W (in.)</u> | <u>h (in.)</u> |
|------------------------------------|----------------|----------------------------|----------------|----------------|----------------|----------------|
| [0] <sub>24</sub>                  | 3.2            | 0.4                        | 1.0            | 0.2            | 0.375          | 0.13           |
| [90] <sub>24</sub>                 | 2.8            | 0.4                        | 1.25           | 0.3            | 0.375          | 0.13           |
| [0 <sub>2</sub> /90] <sub>4s</sub> | 3.2            | 0.4                        | 1.0            | 0.2            | 0.375          | 0.13           |
| [0/90] <sub>6s</sub>               | 3.0            | 0.4                        | 1.5            | 0.25           | 0.375          | 0.13           |
| [90 <sub>2</sub> /0] <sub>4s</sub> | 3.0            | 0.4                        | 0.5            | 0.2            | 0.375          | 0.13           |

TABLE - 2  
 COMPRESSION MECHANICAL PROPERTIES OF AS4/J1  
 THERMOPLASTIC COMPOSITE AT ROOM TEMPERATURE

| <u>Laminates</u>                   | <u>DRY</u>                    |  |                               | <u>WET</u>                    |  |                               |
|------------------------------------|-------------------------------|--|-------------------------------|-------------------------------|--|-------------------------------|
|                                    | <u>E<sub>1</sub></u><br>(Msi) | <u><math>\sigma_{1ucs}</math></u><br>(ksi) | <u>Fatigue limit</u><br>(ksi) | <u>E<sub>1</sub></u><br>(Msi) | <u><math>\sigma_{1ucs}</math></u><br>(ksi) | <u>Fatigue limit</u><br>(ksi) |
| [0] <sub>24</sub>                  | 15.6                          | 98.2                                       | 62.8                          | 15.9                          | 92.5                                       | 66.4                          |
| [0 <sub>2</sub> /90] <sub>4s</sub> | 10.2                          | 70.2                                       | 55.4                          | 11.6                          | 64.6                                       | 56.5                          |
| [0/90] <sub>6s</sub>               | 7.8                           | 60.5                                       | 48.9                          | 7.5                           | 61.4                                       | 49.9                          |
| [90 <sub>2</sub> /0] <sub>4s</sub> | 5.0                           | 46.6                                       | 36.3                          | 4.9                           | 47.9                                       | 30.8                          |
| [90] <sub>24</sub>                 | 0.93                          | 19.5                                       | 11.9                          | 0.95                          | 17.1                                       | 7.6                           |

TABLE - 3  
 COMPRESSIVE YOUNG'S MODULI AND STRENGTHS OF  
 24-PLY AS4/J1 LAMINATES WITH VARIOUS LAYUPS (IITRI TEST FIXTURES)

| <u>Laminates</u>                   | <u>E<sub>1</sub> (Msi)</u> | <u>σ<sub>1ucs</sub> (ksi)</u> |
|------------------------------------|----------------------------|-------------------------------|
| [0] <sub>24</sub>                  | 13.67                      | 111.67                        |
| [0 <sub>2</sub> /90] <sub>4s</sub> | 9.05                       | 82.92                         |
| [0/90] <sub>6s</sub>               | 6.90                       | 65.85                         |
| [90 <sub>2</sub> /0] <sub>4s</sub> | 4.62                       | 50.31                         |
| [90] <sub>24</sub>                 | 0.74                       | 18.22                         |

TABLE - 4  
 AS4/J1 SECTIONING OF THICK THERMOPLASTIC COMPOSITE  
 COMPRESSION MECHANICAL PROPERTIES AT ROOM TEMPERATURE

| <u>Laminates</u> | <u>END</u>                    |                                  |   | <u>MIDDLE</u>                 |                                  |   | <u>CENTER</u>                 |                                  |   |
|------------------|-------------------------------|----------------------------------|---|-------------------------------|----------------------------------|---|-------------------------------|----------------------------------|---|
|                  | <u>E<sub>1</sub></u><br>(Msi) | <u>σ<sub>1ucs</sub></u><br>(ksi) | <u>Fatigue</u><br><u>limit</u><br>(ksi) | <u>E<sub>1</sub></u><br>(Msi) | <u>σ<sub>1ucs</sub></u><br>(ksi) | <u>Fatigue</u><br><u>limit</u><br>(ksi) | <u>E<sub>1</sub></u><br>(Msi) | <u>σ<sub>1ucs</sub></u><br>(ksi) | <u>Fatigue</u><br><u>limit</u><br>(ksi) |
| [0°]             | 15.2                          | 99.1                             | 59.3                                    | 15.9                          | 105.7                            | 55.6                                    | 15.2                          | 103.3                            | 55.6                                    |
| [90°]            | 0.92                          | 21.4                             | 11.8                                    | 0.96                          | 21.1                             | ----                                    | 0.90                          | 20.3                             | 13.1                                    |

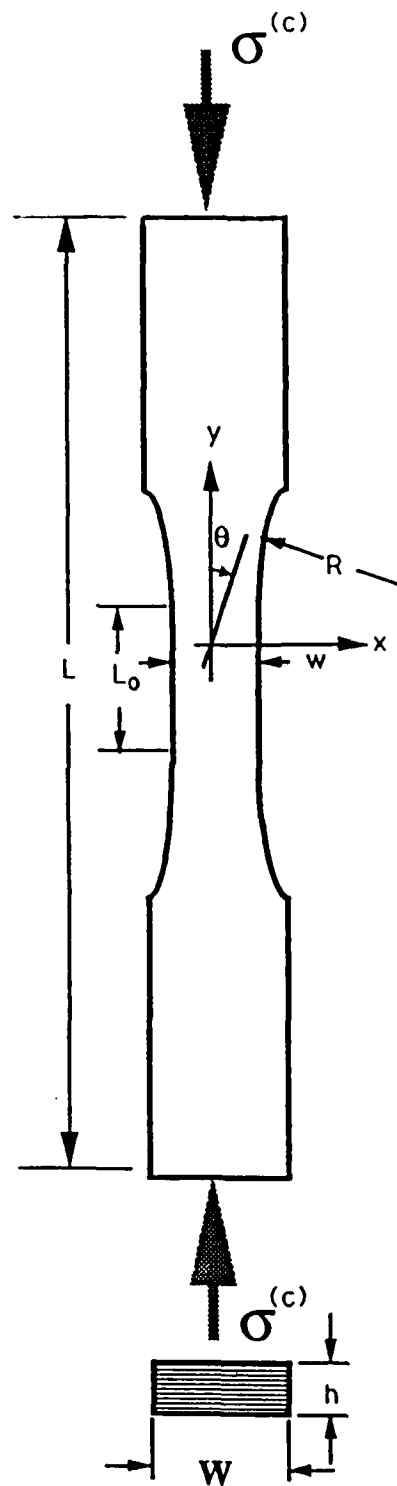
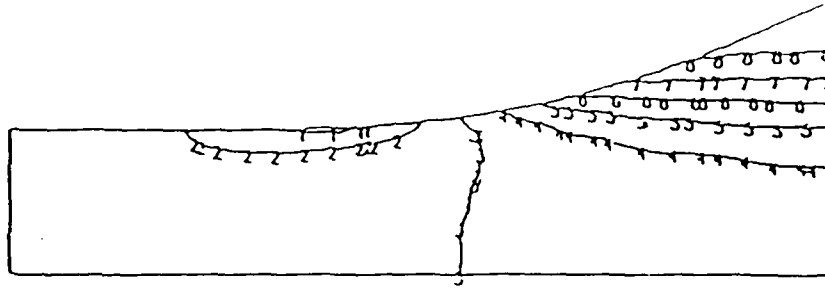


Fig. 1 Specimen Geometry Used for Studying Compressive Fatigue of AS4/Polyamide Thermoplastic Composite.

S11

VALUE

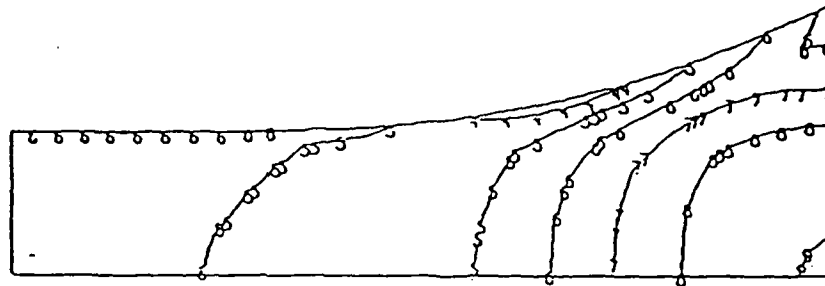
- |    |           |
|----|-----------|
| 1  | -3.00E+06 |
| 2  | -2.00E+06 |
| 3  | -2.20E+06 |
| 4  | -1.80E+06 |
| 5  | -1.40E+06 |
| 6  | -1.00E+06 |
| 7  | -6.00E+05 |
| 8  | -1.99E+05 |
| 9  | +2.00E+05 |
| 10 | +6.00E+05 |
| 11 | +1.00E+06 |



S22

VALUE

- |    |           |
|----|-----------|
| 1  | -1.00E+05 |
| 2  | -8.00E+04 |
| 3  | -6.00E+04 |
| 4  | -4.00E+04 |
| 5  | -1.99E+04 |
| 6  | +2.00E+02 |
| 7  | +2.00E+04 |
| 8  | +4.00E+04 |
| 9  | +6.00E+04 |
| 10 | +8.00E+04 |
| 11 | +1.00E+05 |



S12

VALUE

- |    |           |
|----|-----------|
| 1  | -3.00E+05 |
| 2  | -2.60E+05 |
| 3  | -2.20E+05 |
| 4  | -1.80E+05 |
| 5  | -1.40E+05 |
| 6  | -1.00E+05 |
| 7  | -6.00E+04 |
| 8  | -1.99E+04 |
| 9  | +2.00E+04 |
| 10 | +6.00E+04 |
| 11 | +1.00E+05 |

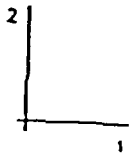
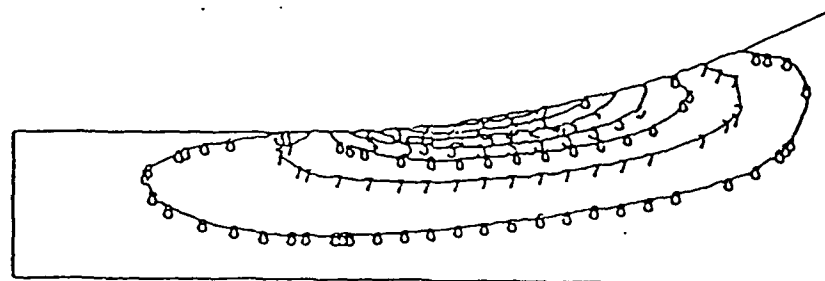


Fig. 2 Isostress Contours in a  $[0]_{24}$  Composite Specimen under  $\delta_1 = -0.08$ .  
 (a)  $\sigma_{11}$ , (b)  $\sigma_{22}$  and (c)  $\sigma_{33}$ .

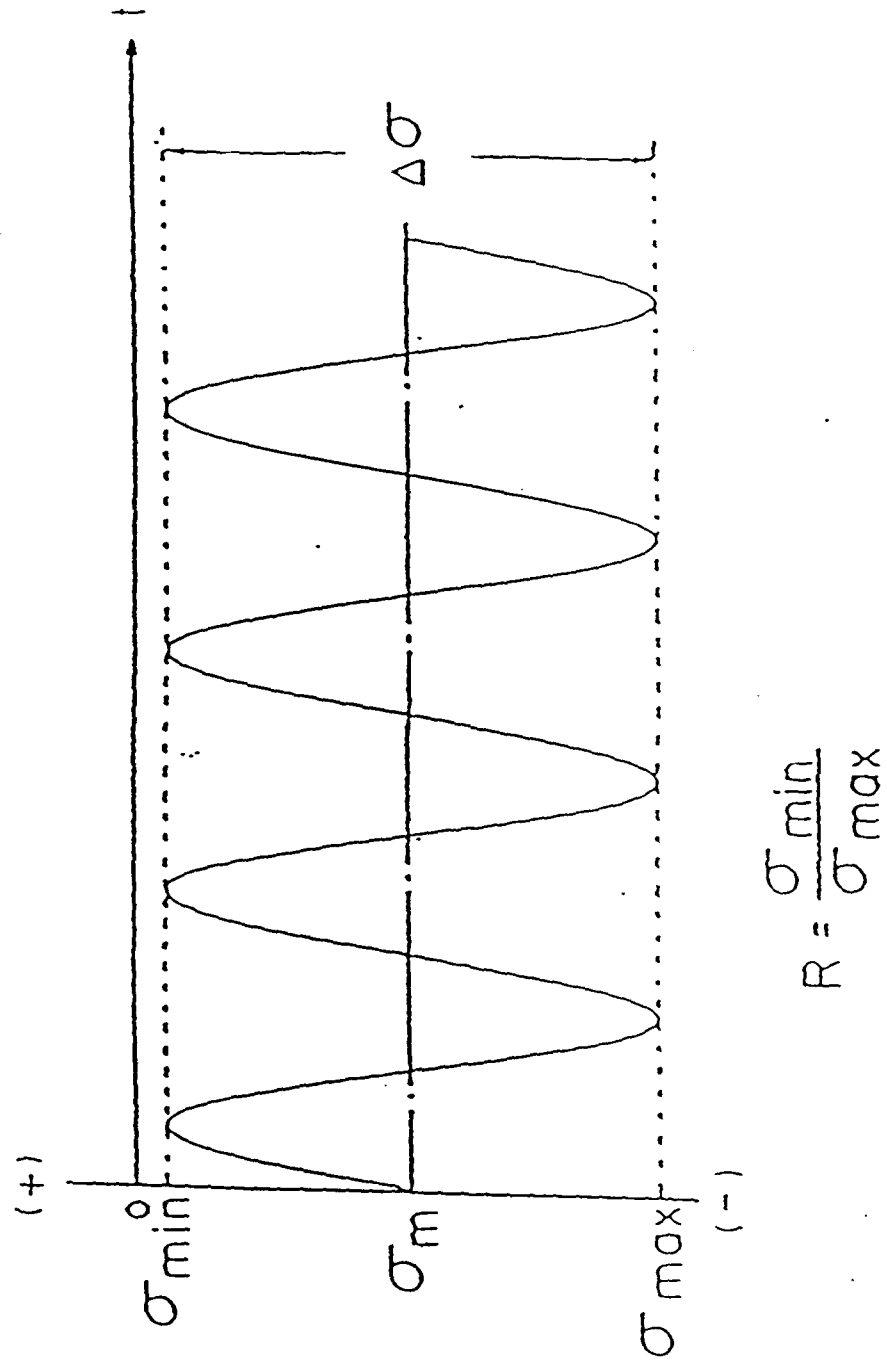


Fig. 3 Compressive Fatigue Load Function Used in the Experiment.



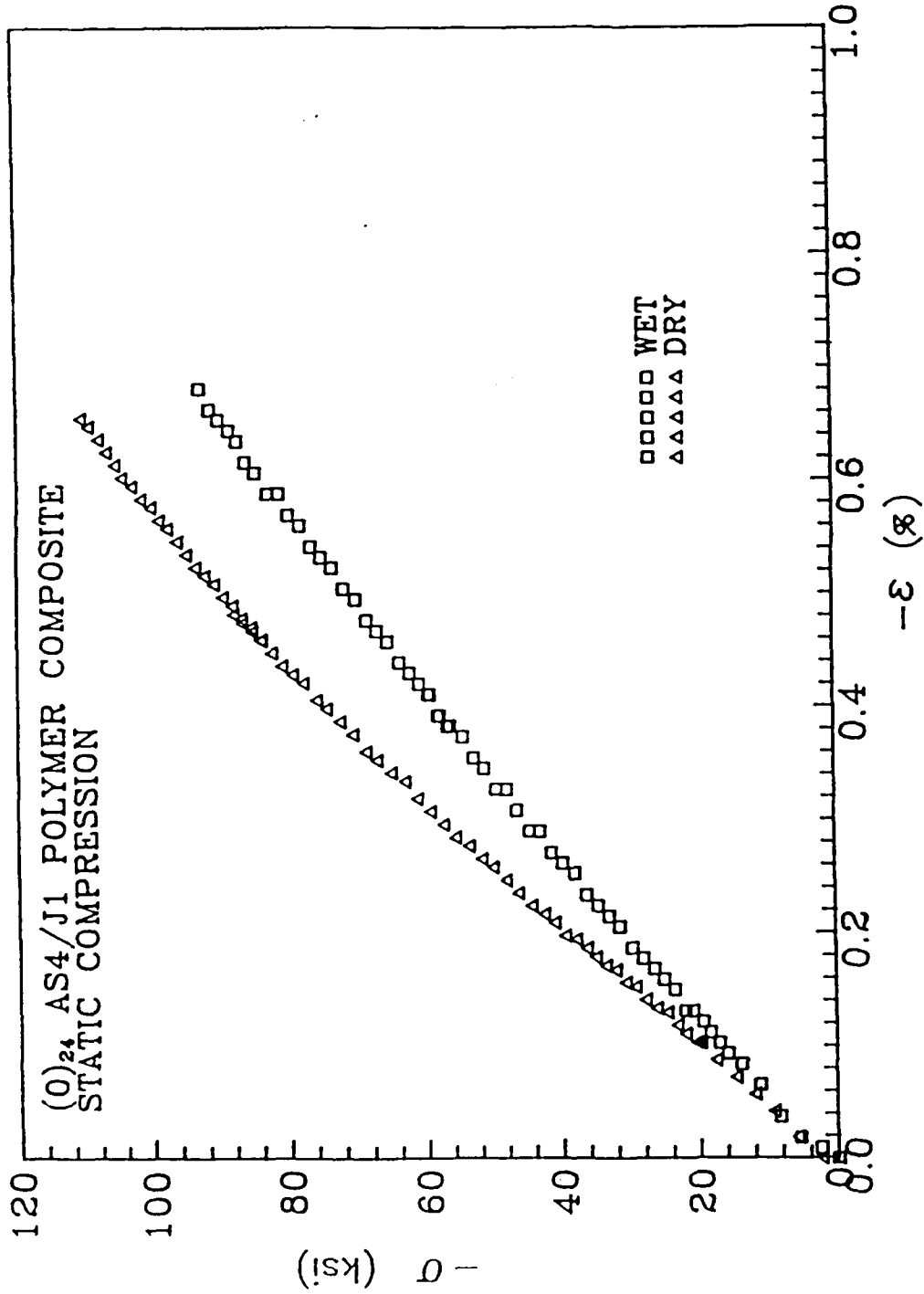


Fig. 4 Compressive Stress-Strain Behavior of (0)<sub>24</sub> AS4/Polyamide Thermoplastic Composite in Ambient and Water-Saturated Environments.

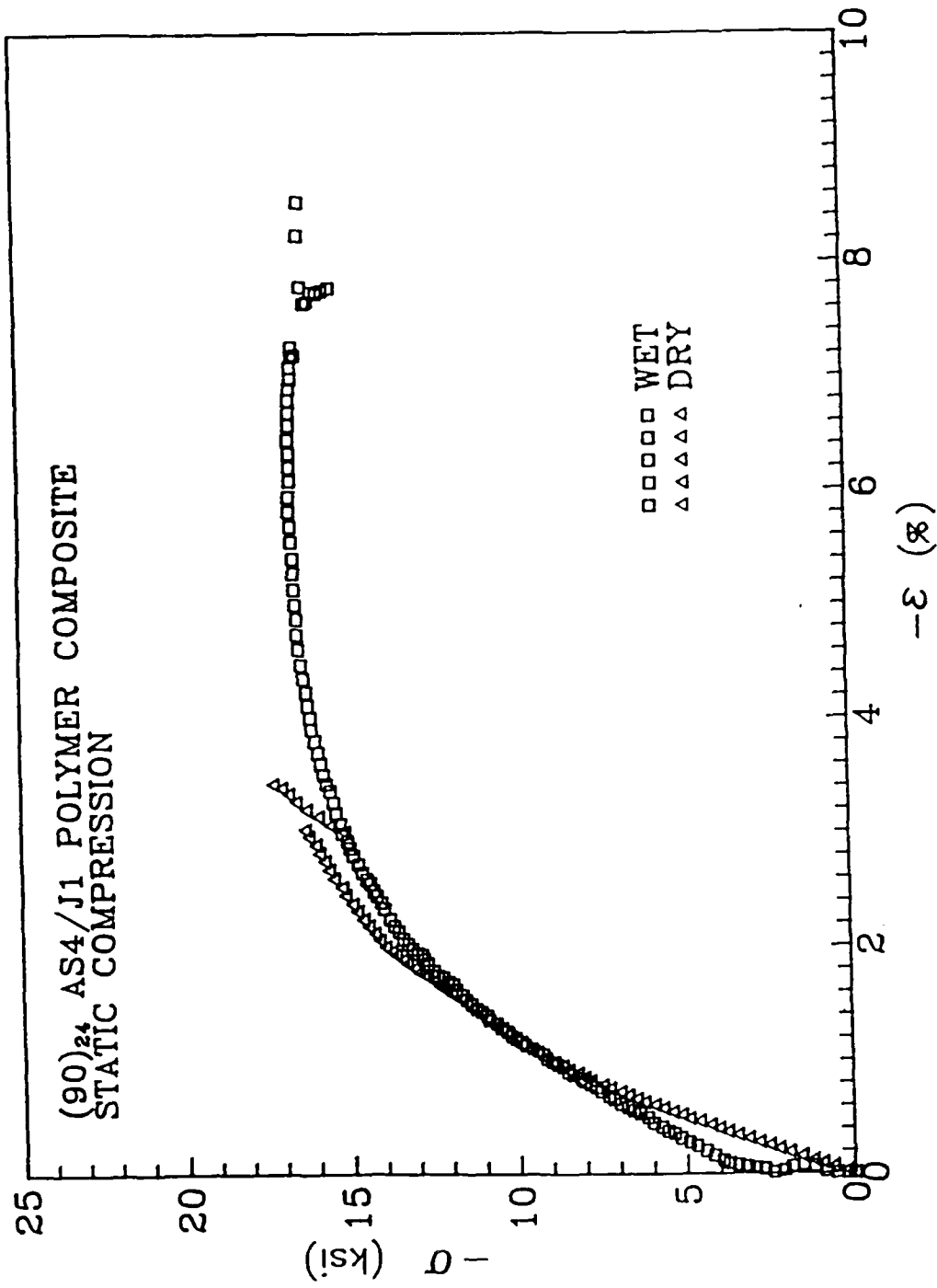


Fig. 5 Compressive Stress-Strain Behavior of [90]<sub>24</sub> AS4/Polyamide Thermoplastic Composite in Ambient and Water-Saturated Environments.

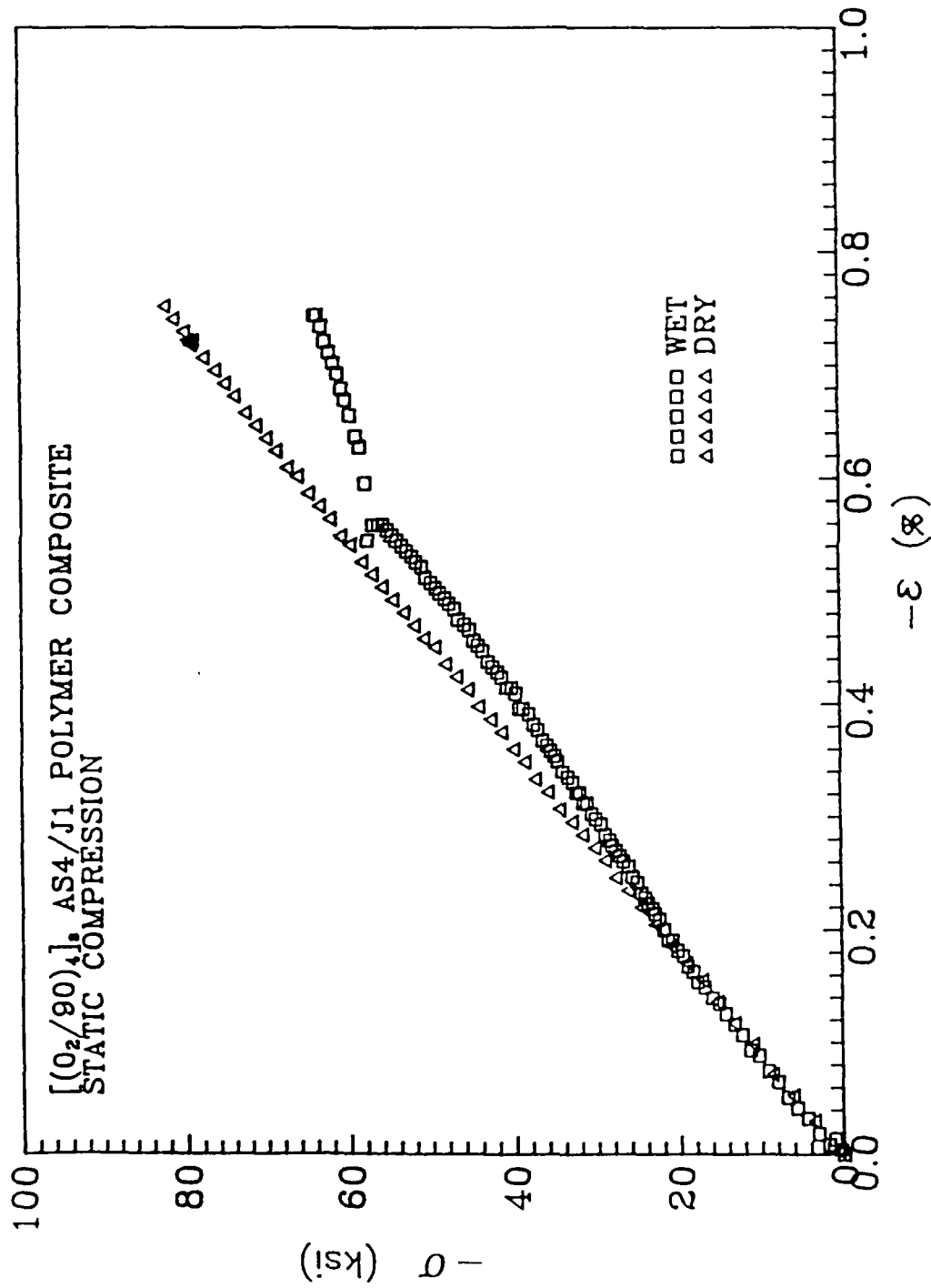


Fig. 6 Compressive Stress-Strain Behavior of [(O<sub>2</sub>/90)<sub>4</sub>]<sub>s</sub> Crossply AS4/Polyamide Thermoplastic Composite in Ambient and Water-Saturated Environments.

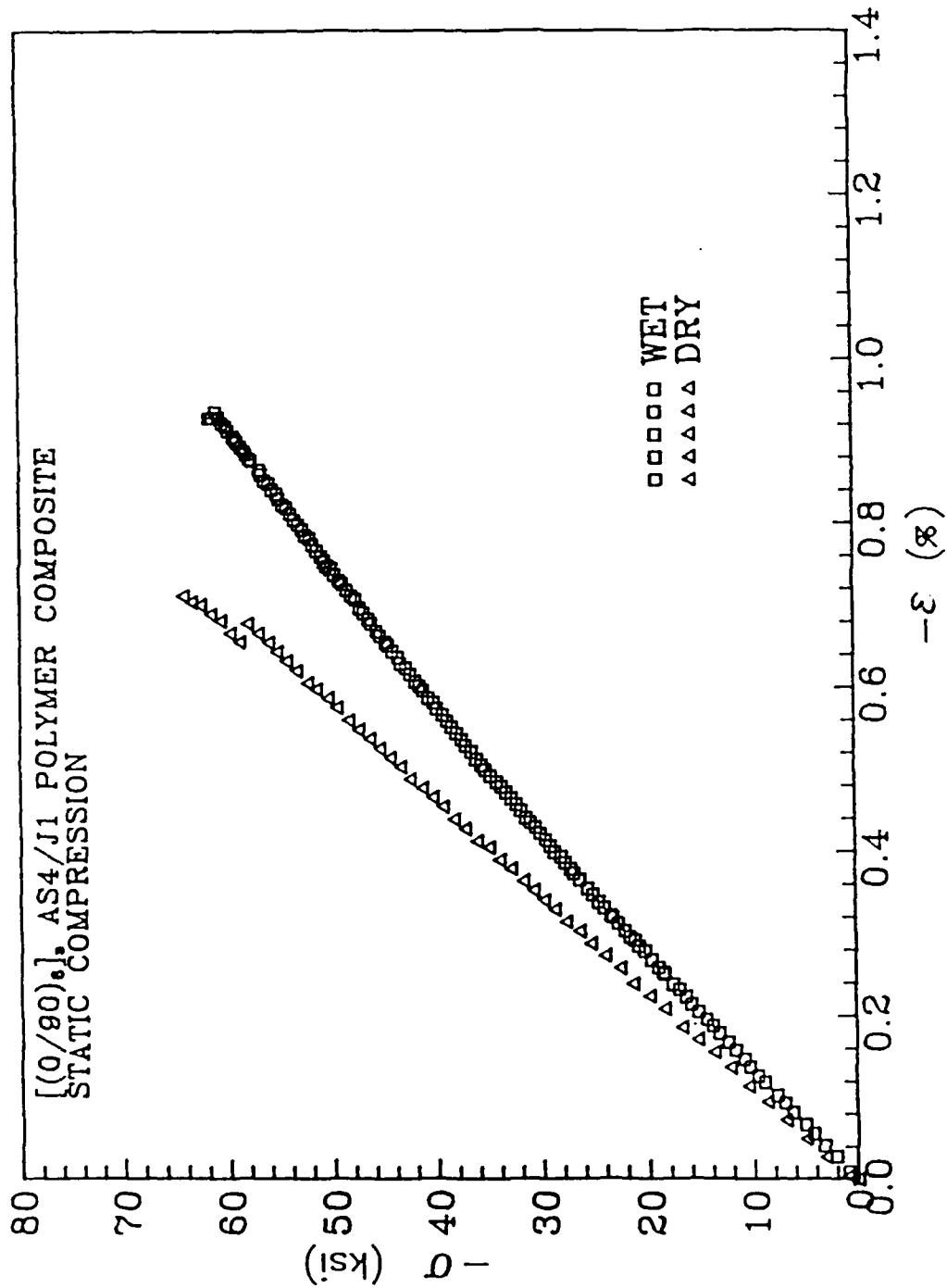


Fig. 7 Compressive Stress-Strain Behavior of  $[(0/90)_6]$  Crossply AS4/Polyamide Thermoplastic Composite in Ambient and Water-Saturated Environments.

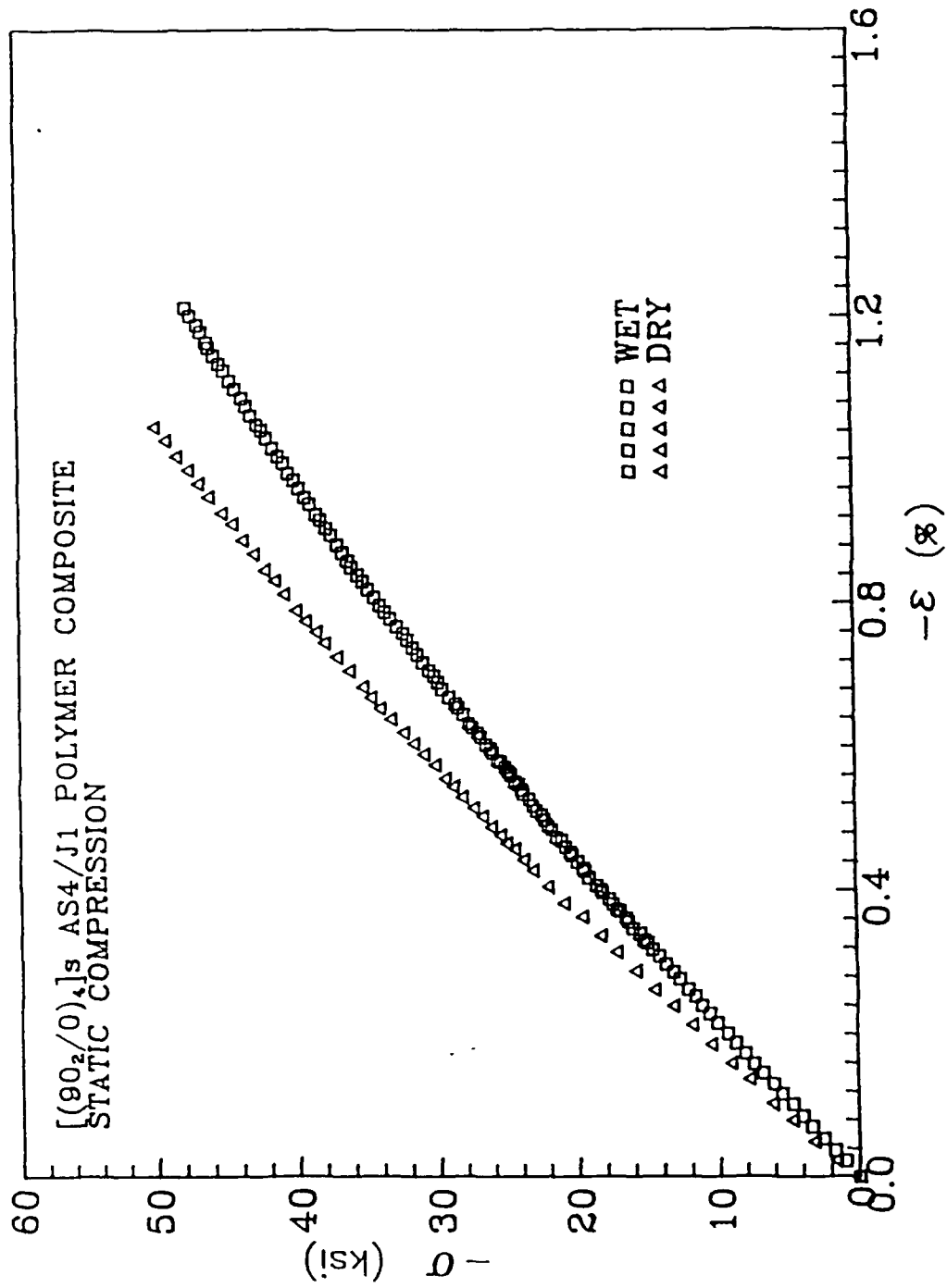


Fig. 8 Compressive Stress-Strain Behavior of [(90<sub>2</sub>/0)<sub>4</sub>]<sub>s</sub> Crossply AS4/Polyamide Thermoplastic Composite in Ambient and Water-Saturated Environments.

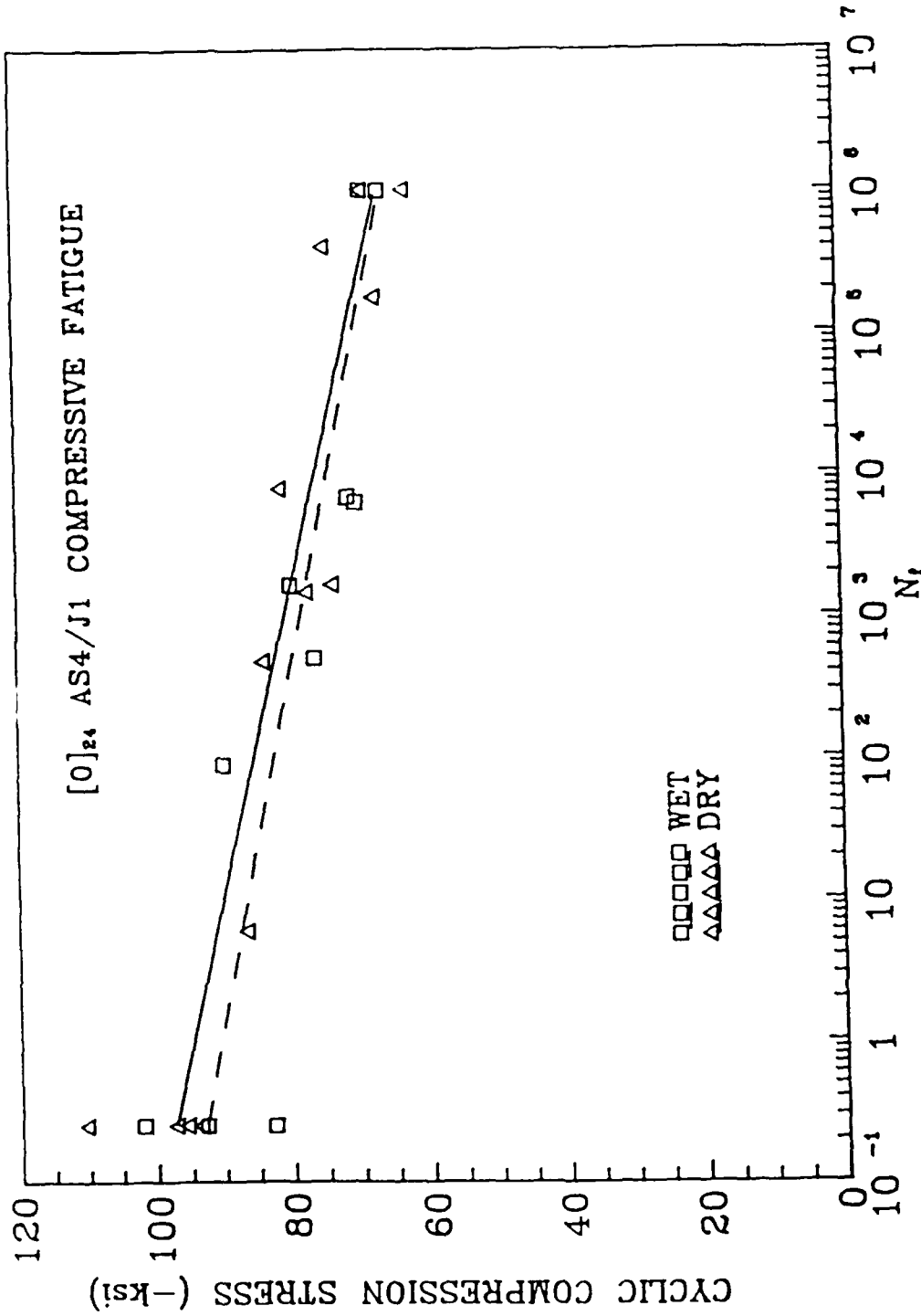


Fig. 9 Cyclic Compressive S- $N_f$  Diagram for [0]<sub>24</sub> AS4/Polyamide Thermoplastic Composite in Ambient and Water-Saturated Environments.

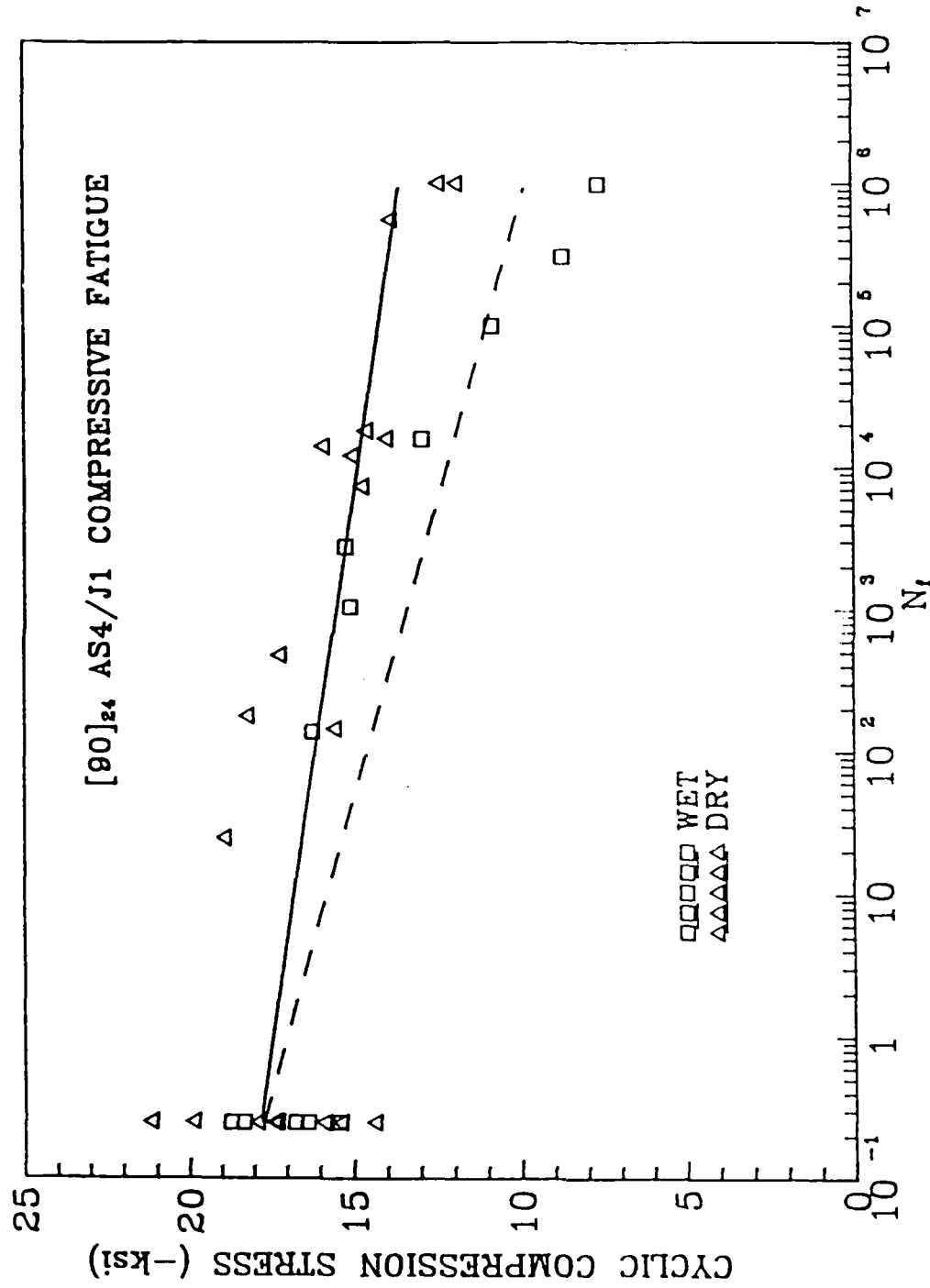


Fig. 10 Cyclic Compressive S- $N_f$  Diagram for [90]<sub>24</sub> AS4/Polyamide Thermoplastic Composite in Ambient and Water-Saturated Environments.

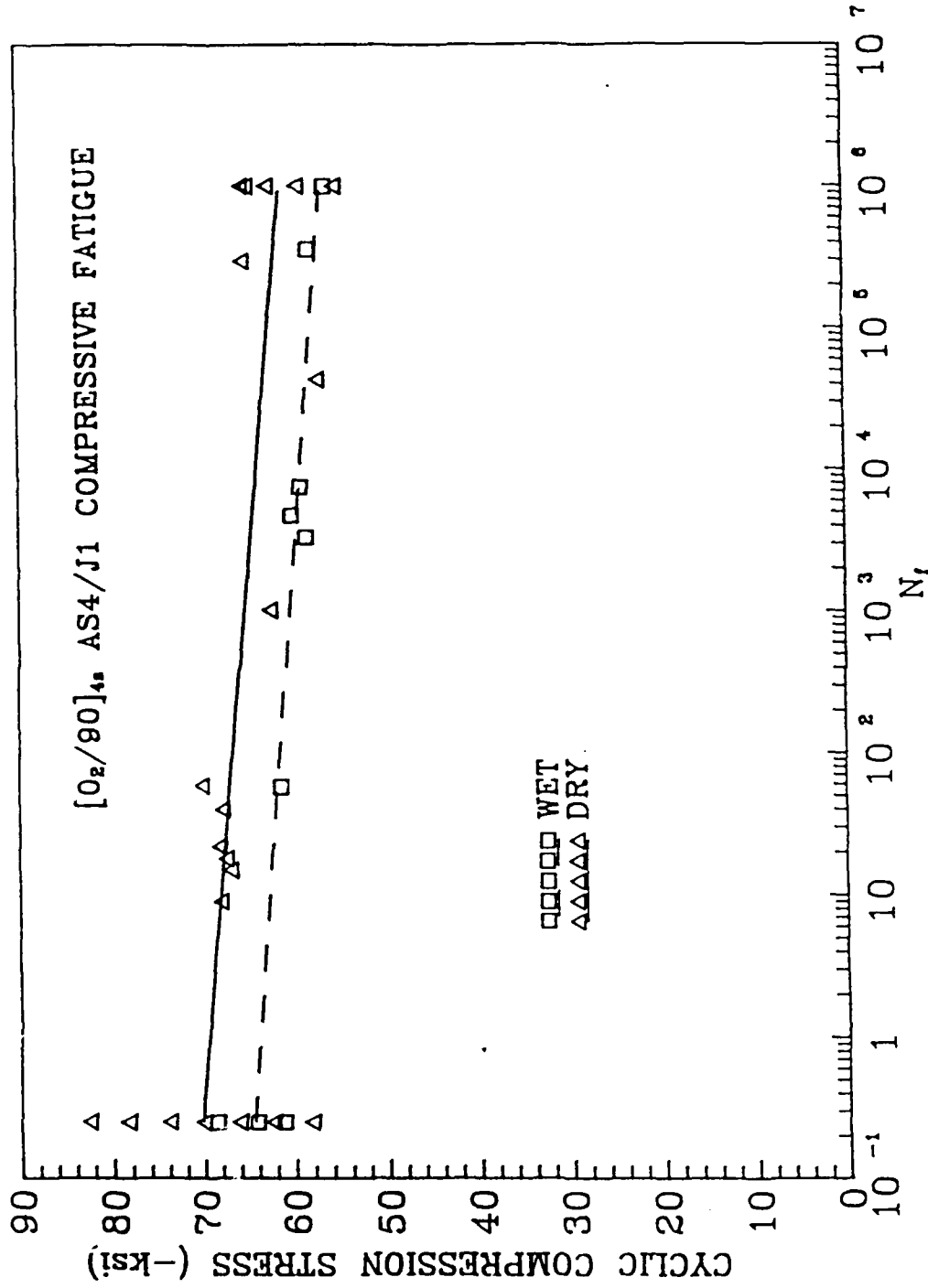


Fig. 11 Cyclic Compressive S- $N_f$  Diagram for  $[0_2/90]_{4s}$  Crossply AS4/Polyamide Thermoplastic Composite in Ambient and Water-Saturated Environments.



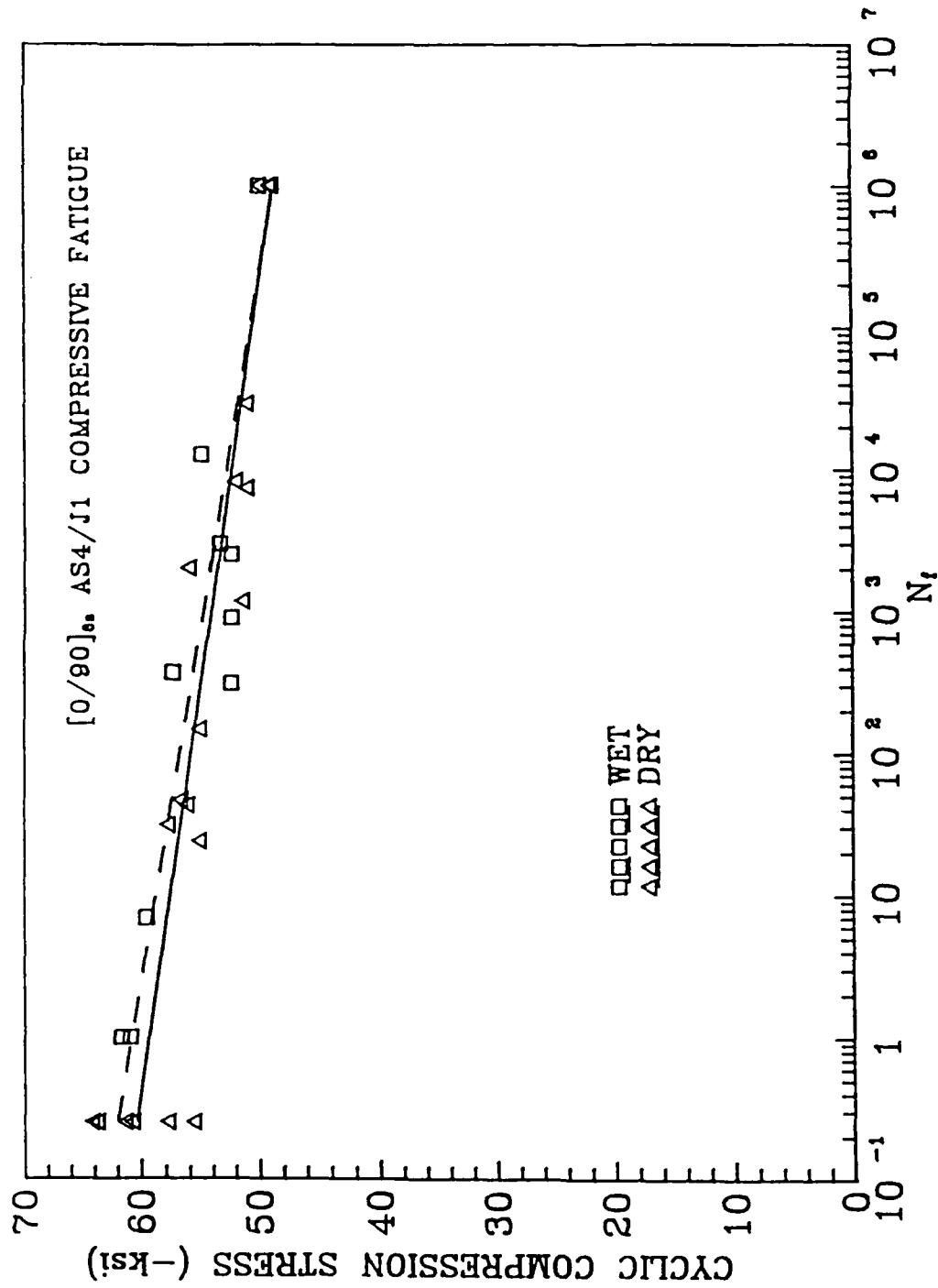


Fig. 12 Cyclic Compressive S- $N_f$  Diagram for [0/90]<sub>6s</sub> Crossply AS4/Polyamide Thermoplastic Composite in Ambient and Water-Saturated Environments.

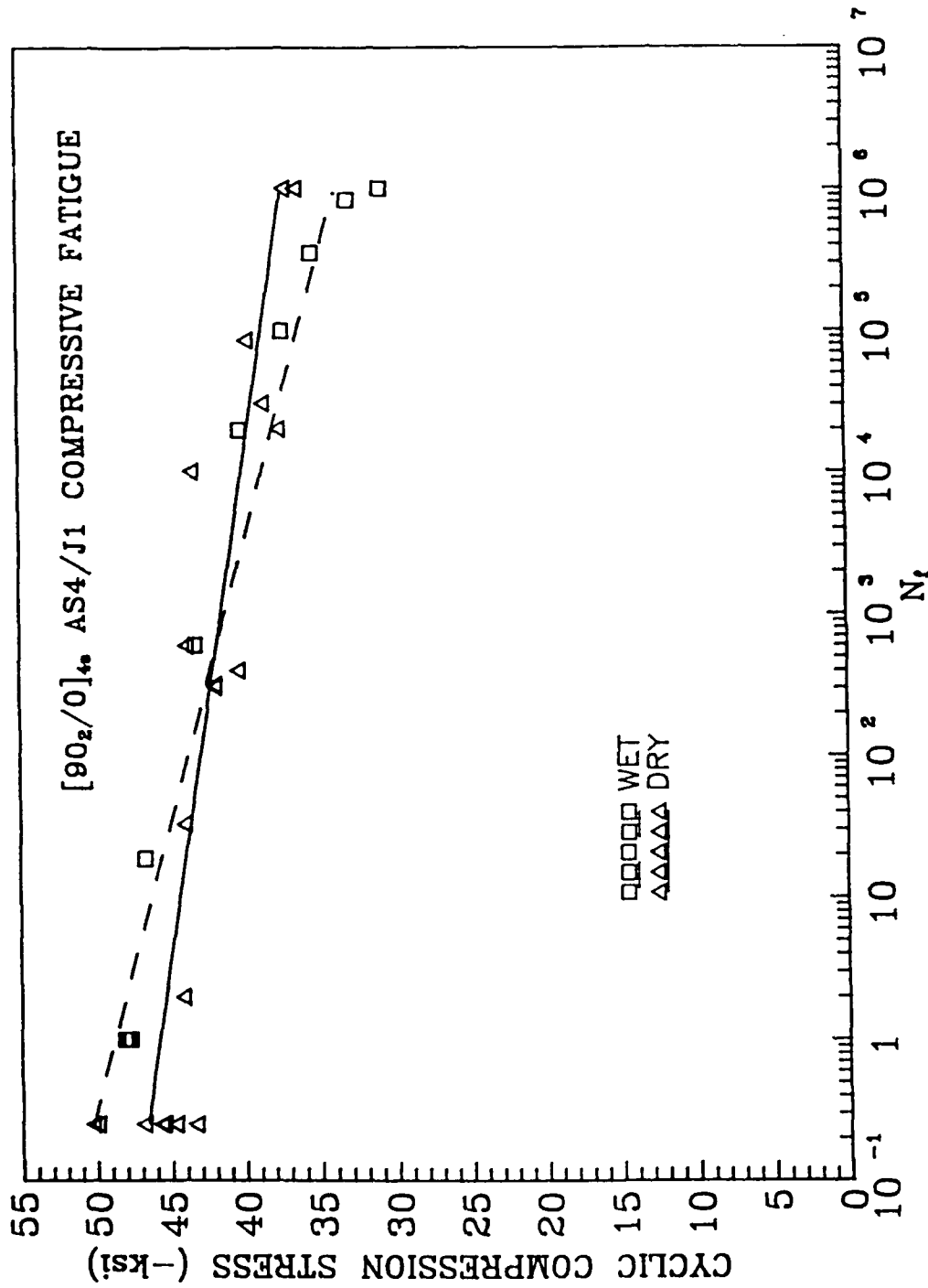


Fig. 13 Cyclic Compressive S- $N_f$  Diagram for  $[90_2/0]_{4s}$  Crossply AS4/Polyamide Thermoplastic Composite in Ambient and Water-Saturated Environments.

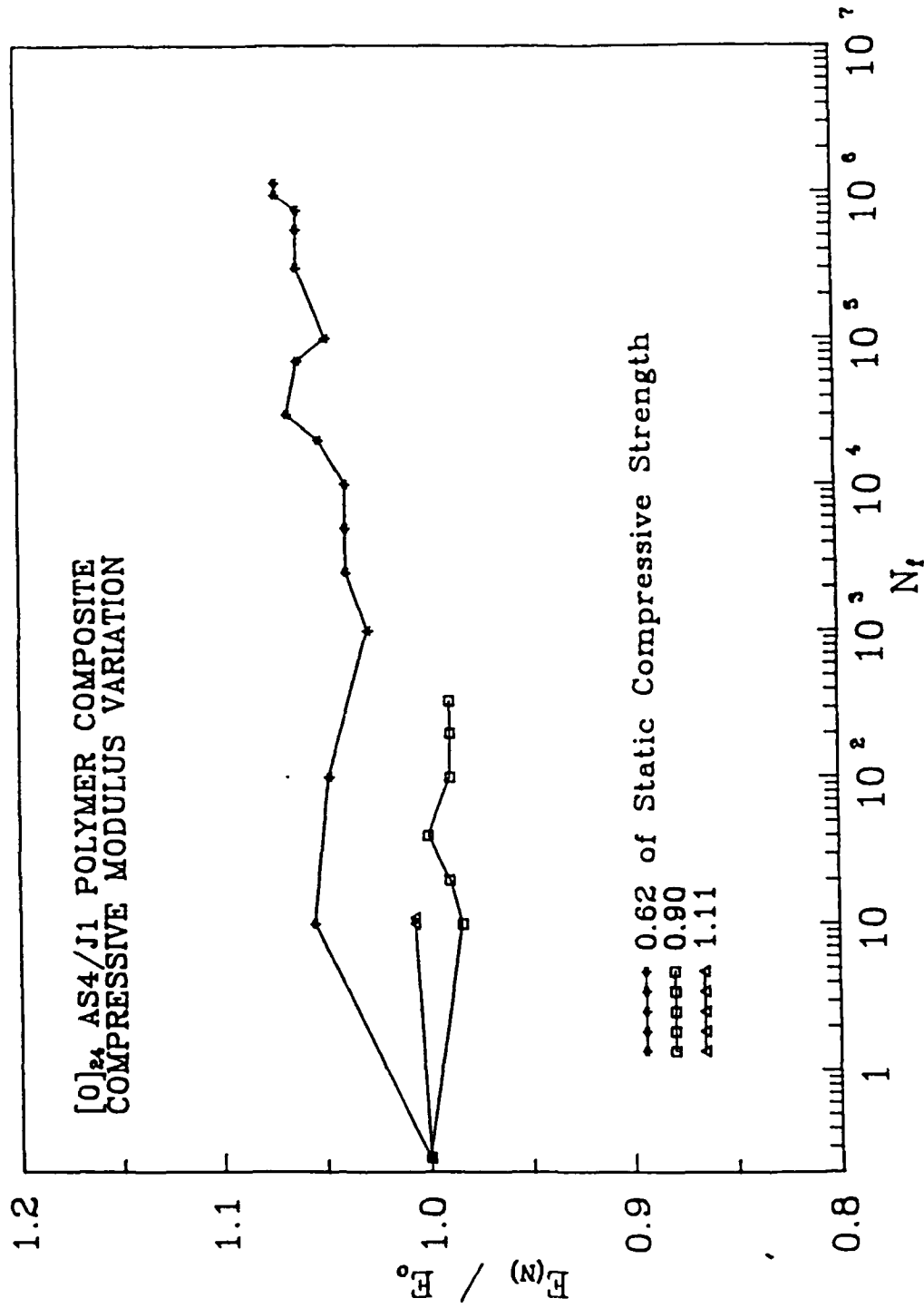


Fig. 14 Variation of Compressive Modulus of [0]<sub>24</sub> AS4/Polyamide Thermoplastic Composite in Ambient Environment During Cyclic Compressive Fatigue at Three Cyclic Stress Levels .

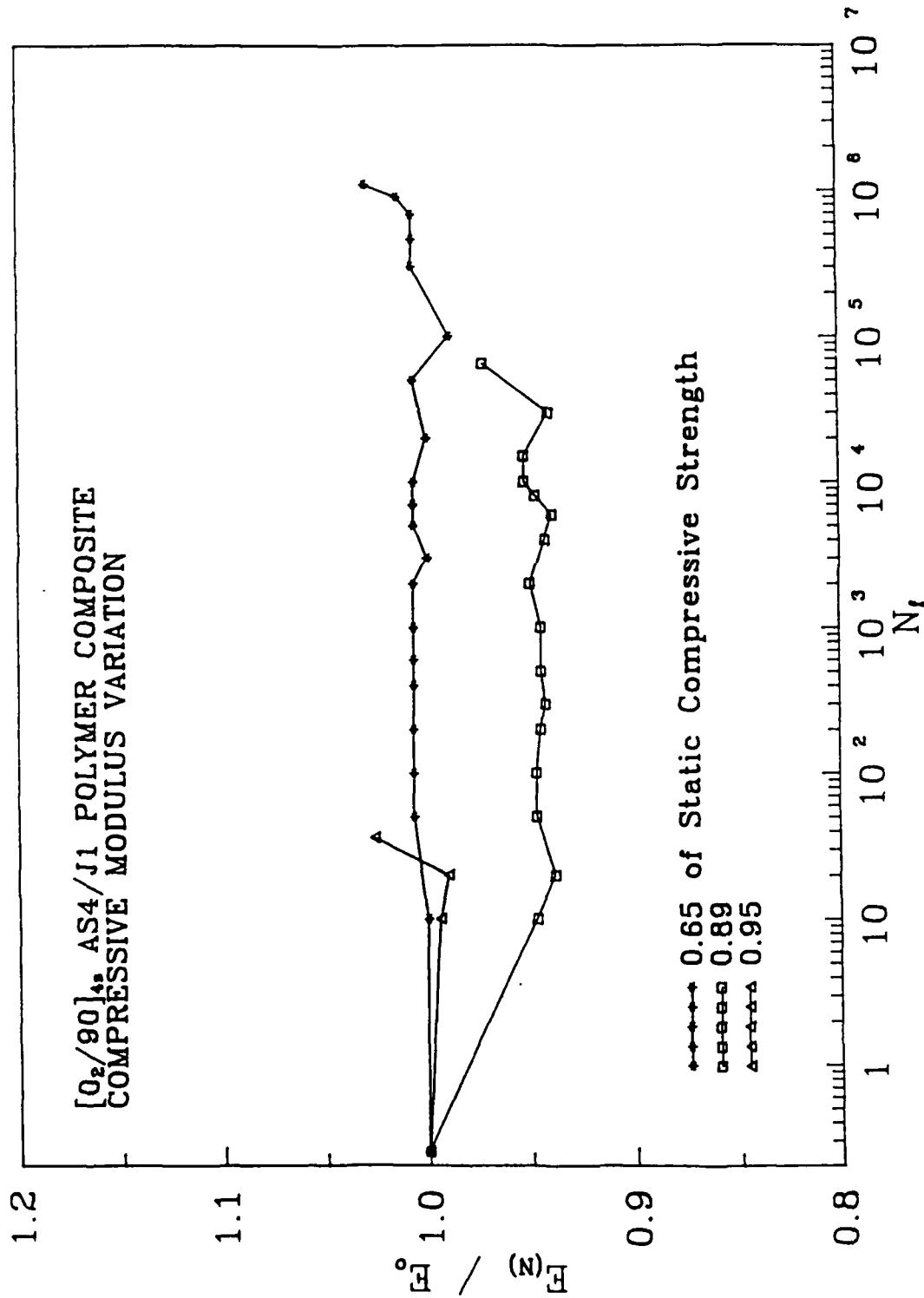


Fig. 15 Variation of Compressive Stiffness of [0<sub>2</sub>/90]<sub>4s</sub> Crossply AS4/Polyamide Thermoplastic Composite in Ambient Environment During Cyclic Compressive Fatigue at Three Cyclic Stress Levels.

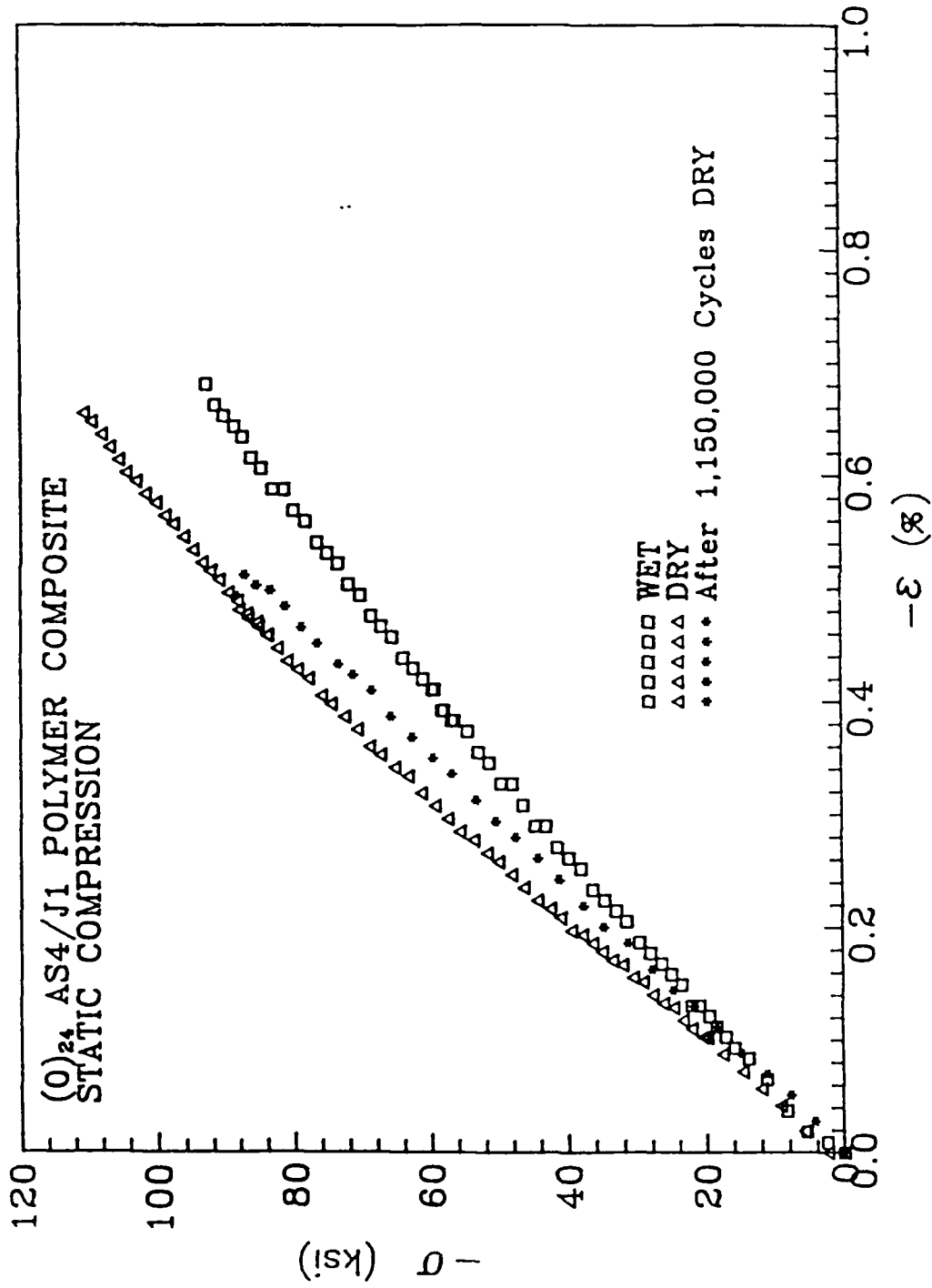


Fig. 16 Compressive Stress-Strain Behavior of [0]<sub>24</sub> AS4/Polyamide Thermoplastic Composite Before and After Cyclic Compressive Fatigue.

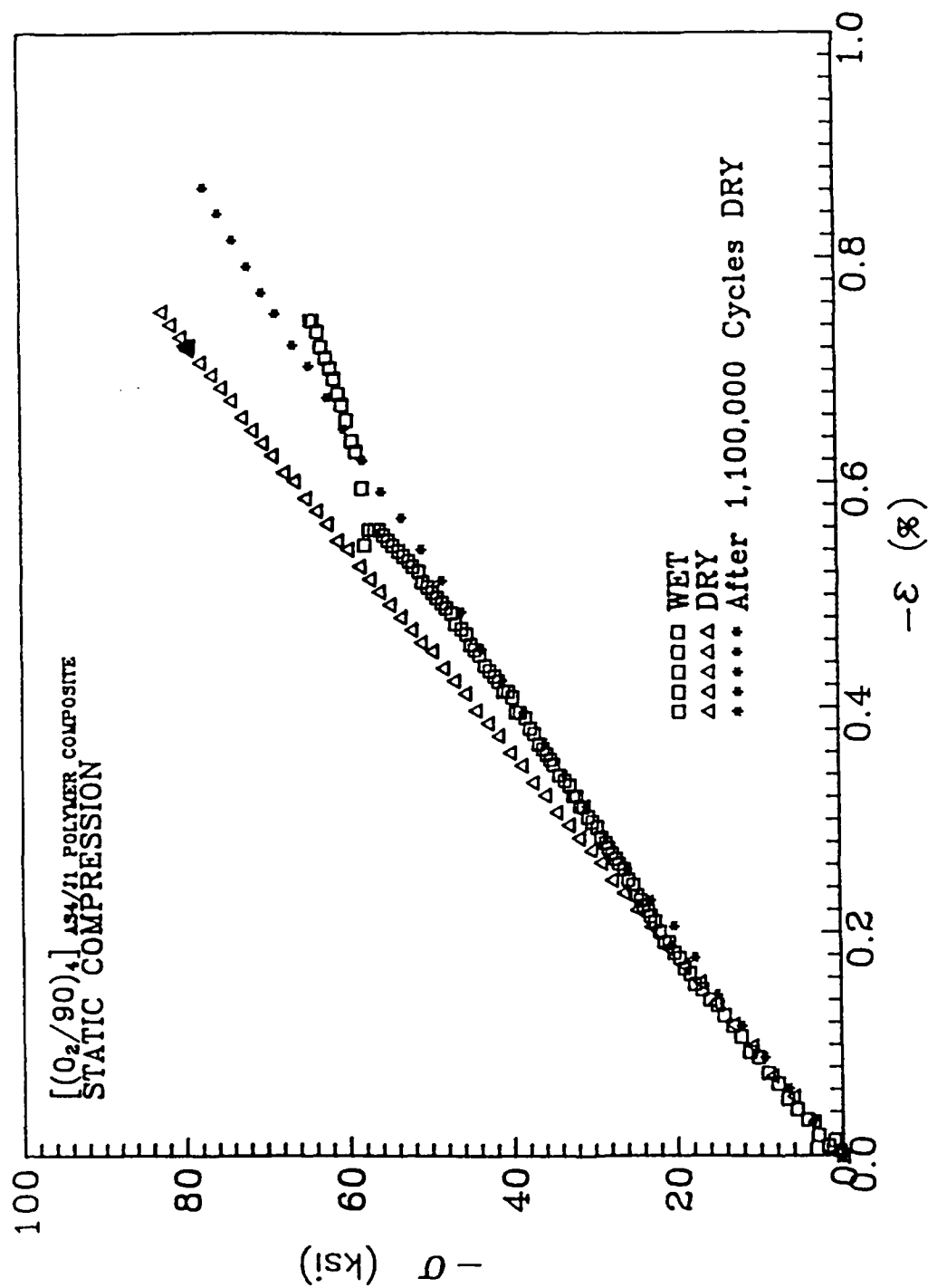


Fig. 17 Compressive Stress-Strain Behavior of  $[(0_2/90)_4]_{AS4}$  Crossply AS4/Polyamide Thermoplastic Composite Before and After Cyclic Compressive Fatigue.

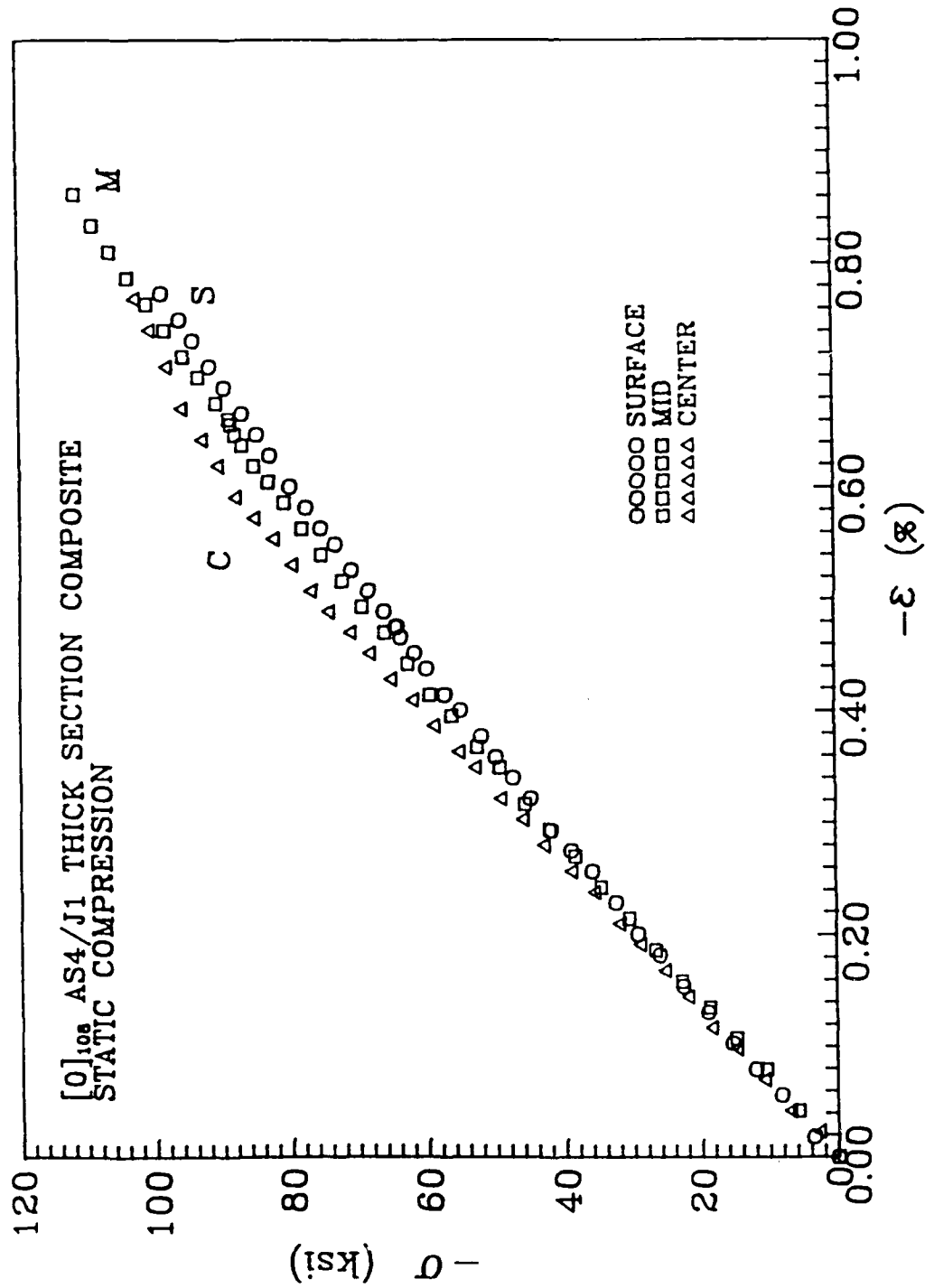


Fig. 18 Compressive Stress-Strain Behavior at Different Thickness Positions of a Thick [0]<sub>108</sub> AS4/Polyamide Thermoplastic Composite in Ambient Environment.

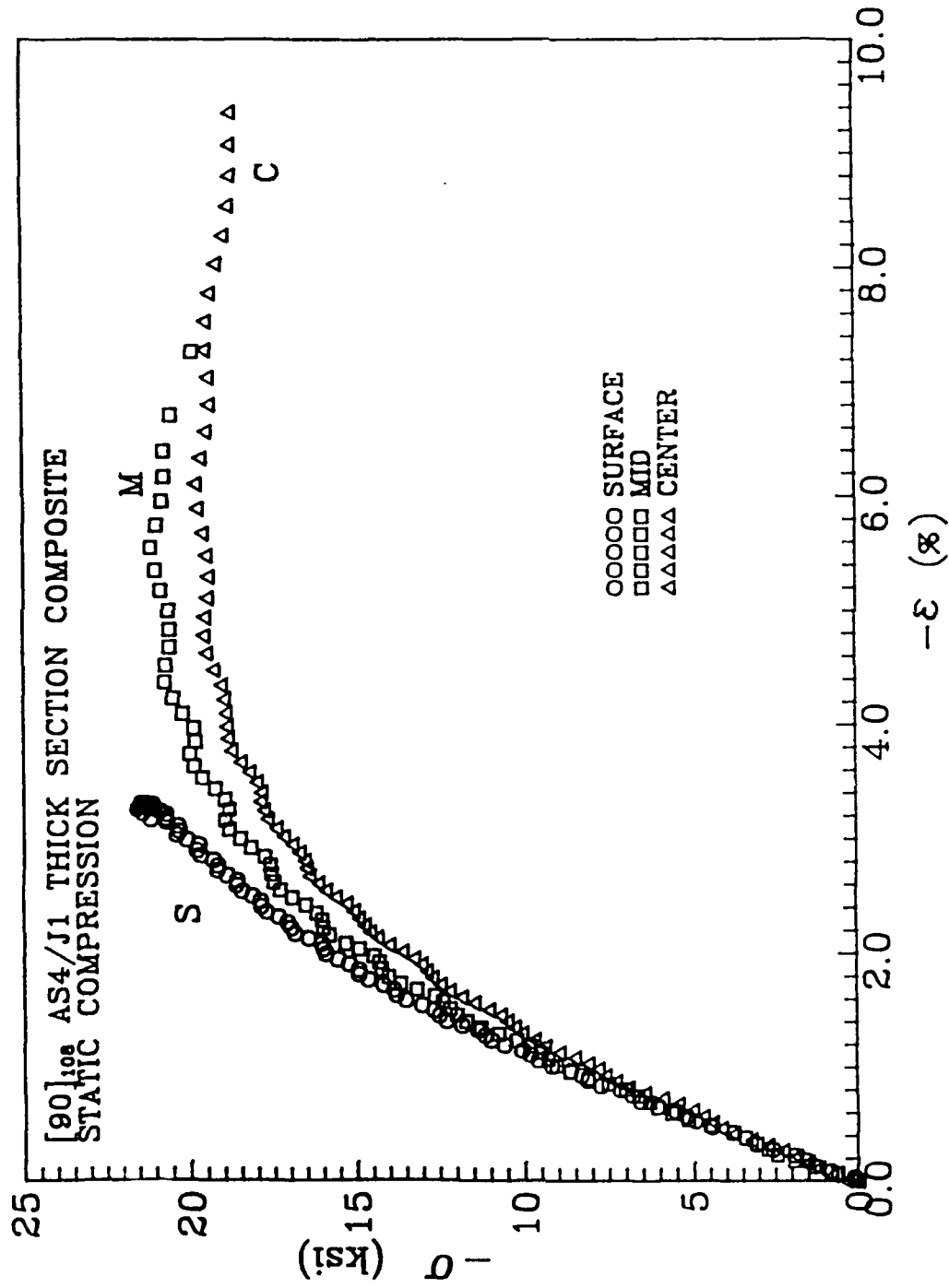


Fig. 19 Compressive Stress-Strain Behavior at Different Thickness Positions of a Thick [90]<sub>108</sub> AS4/Polyamide Thermoplastic Composite in Ambient Environment.



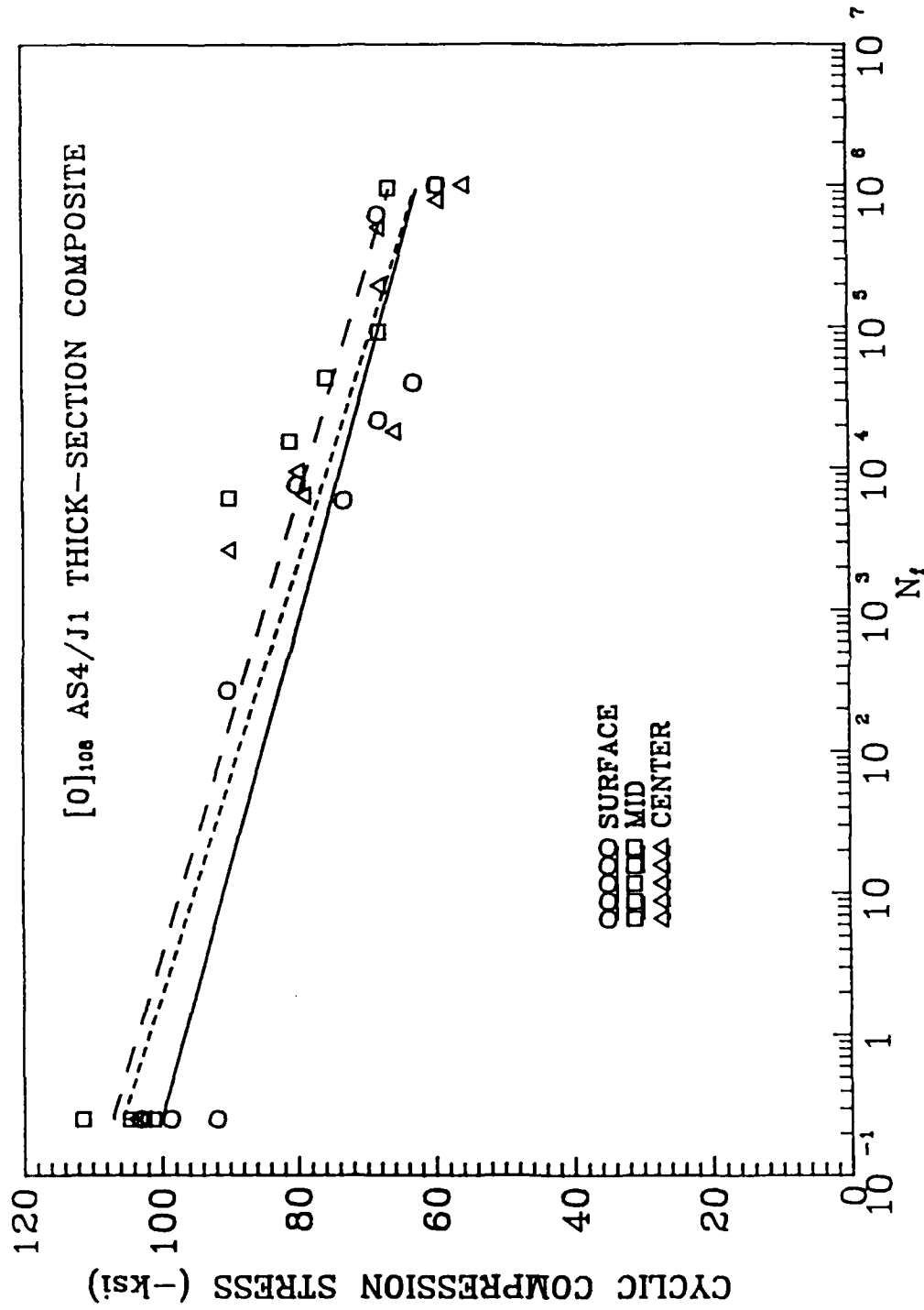


Fig. 20 Cyclic Compressive S-N<sub>f</sub> Behavior for Specimens Sectioned at Different Thickness Locations in a [0]<sub>108</sub> AS4/Polyamide Thermoplastic Composite in Ambient Environment.

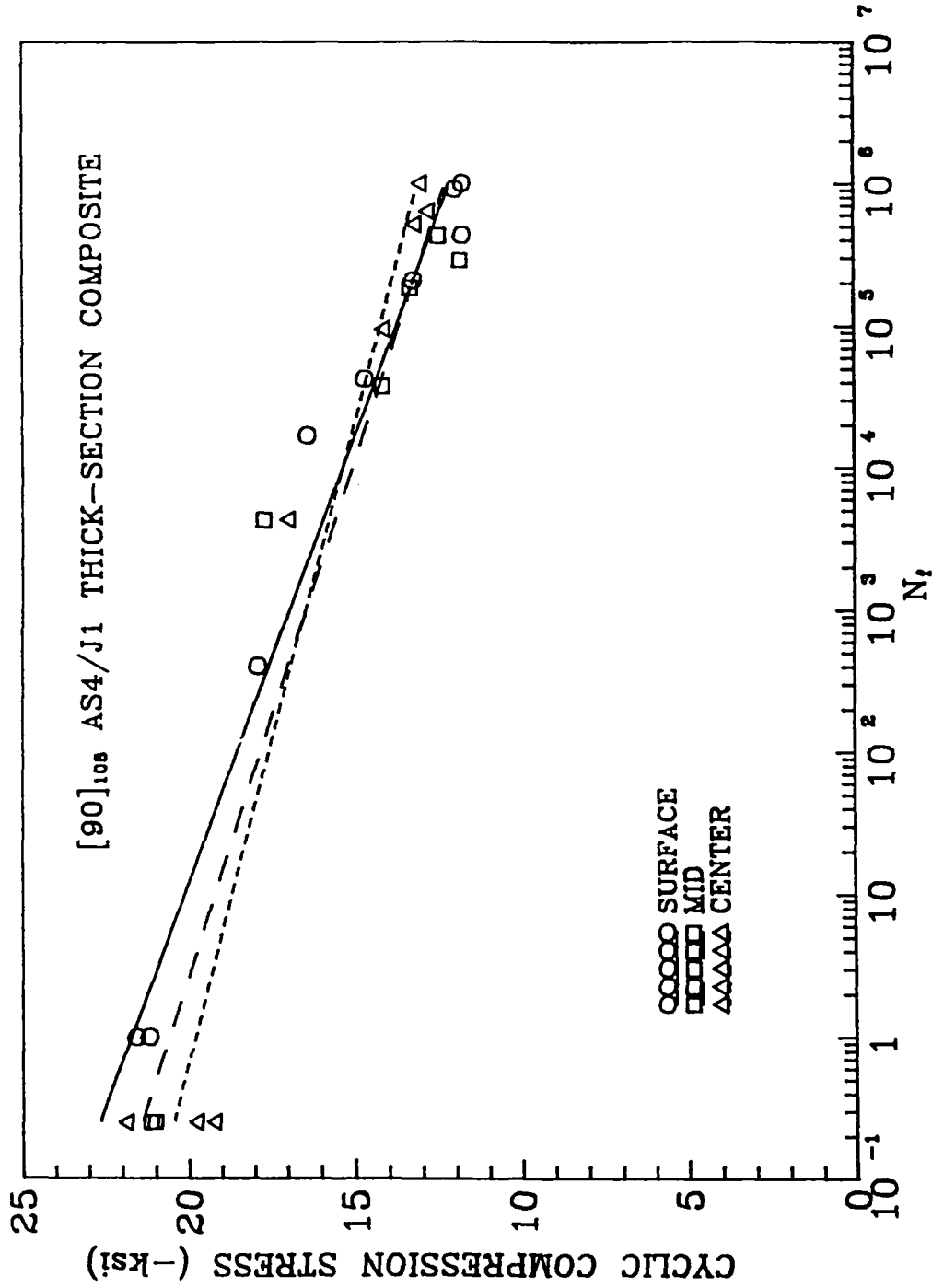


Fig. 21 Cyclic Compressive S- $N_f$  Behavior for Specimens Sectioned at Different Thickness Locations in a [90]<sub>108</sub> AS4/Polyamide Thermoplastic Composite in Ambient Environment.

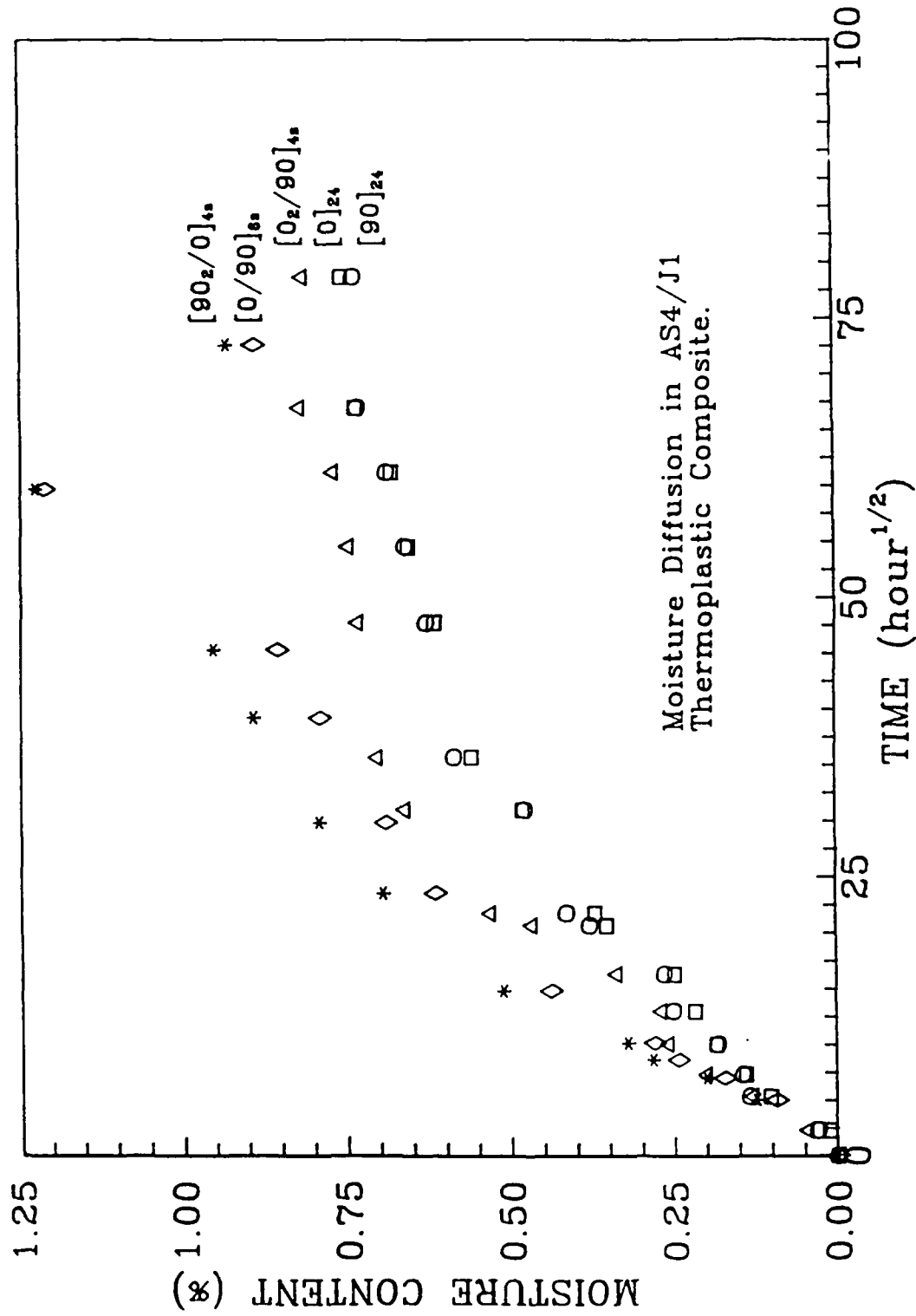


Fig. 22 Moisture Diffusion in AS4/Polyamide Thermoplastic Composite.

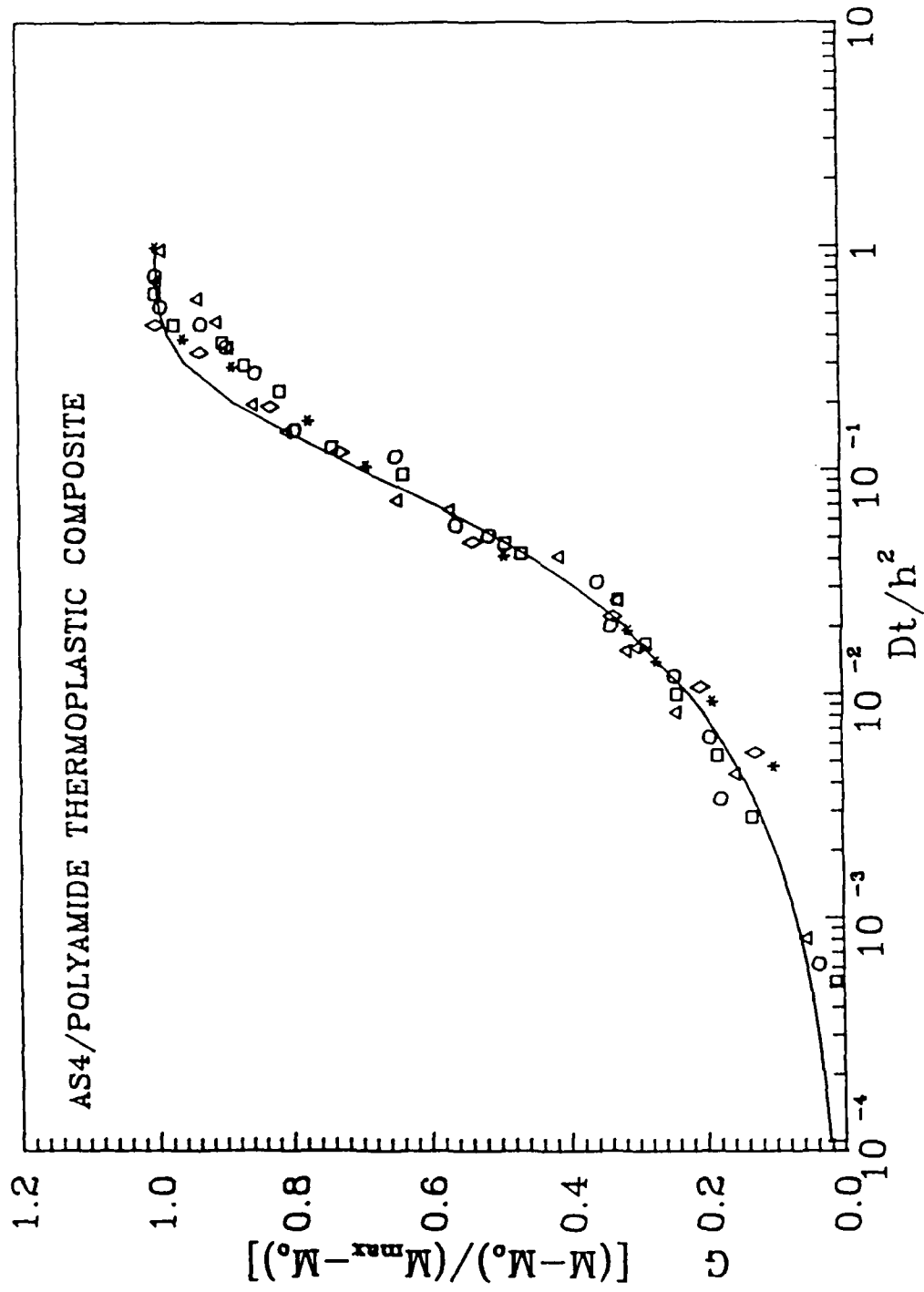


Fig. 23 Comparison of Analytical and Measured Moisture Concentration (G) Values for AS4/Polyamide Thermoplastic Composite.

## REFERENCES

- [1] Marchant, A., Pinzelli, R. F., "Composite for Marine Structures - Where is the Future?", Looking Ahead for Materials and Processes, (J. de Bossu, F. Briens and P. Lissac, Eds.), Elsevier Science Publishers B.V., Amsterdam, 1987, pp. 257-270.
- [2] Chauchot, P., Guillermin, O., "On the Use of Composite Materials for 6000 m Containers Case of the Magnetometer of the S.A.R.", Looking Ahead for Materials and Processes, (J. de Bossu and F. Briens and P. Lissac, Eds.), Elsevier Science Publishers B.V., Amsterdam, 1987, pp. 315-328.
- [3] Hahn, H. T., "Fatigue of Composites: Environmental Effects", Fatigue and Creep of Composite Materials, (H. Liholt, R. Talreja, Eds.), Roskilde, Denmark, 1982, pp. 19-35.
- [4] Gopalan, R., Somashekar B. R., Dattaguru, B.k., "Environmental Effects on Fibre-Polymer Composites", Polymer Degradation and Stability, Vol. 24, No. 4, 1989, pp. 367-371.
- [5] Henrat, P., "Compression Properties of High Performance Composites Tested with Different Methods", Looking Ahead of Materials and Processes, (J. de Bossu, F. Briens and P. Lissac, Eds.), Elsevier Science Publishers B.V., Amsterdam, 1987, pp. 389-399.
- [6] Adist, N. R., "Compression Testing of Graphite/Epoxy", Compression Testing of Homogeneous Materials and Composites, ASTM STP 808, (R. Chait and R. Papirno, Eds.), American Society for Testing and Materials, Philadelphia, PA., 1983, pp. 175-186.
- [7] Kim, R. Y., Tsai, S. W., "A Compressive Test Method For Ring Specimens", Proceedings of the 33rd International SAMPE Symposium, (G. Carrillo, E. D. Newell, W. D. Brown and P. Phelan, Eds.), Society for the Advancement of Material and Process Engineering, 1988, pp. 1159-1168.
- [8] Muzzy, J. D., and Kays, A. O., "Thermoplastic vs. Thermosetting Structural Composites", Polymer Composites, Vol. 5, No. 3, 1984, pp. 169-172.
- [9] Lustiger, A., "Considerations in the Utilization of Semicrystalline Thermoplastic Advanced Composites", SAMPE Journal, Vol. 20, No. 5, 1984, pp. 13-16.
- [10] Willats, D., "Advances in the Use of High Performance Continuous Fibre Reinforced Thermoplastics", SAMPE Journal, Vol. 20, No. 5, 1984, pp.6-10.
- [11] Wang, S. S., "A Literature Review on Compressive Deformation and Failure of Fiber Composite Materials", NCCMR Technical Report, National Center for Composite Materials Research, Urbana, IL, 1990.

- [12] Camponeschi, Jr. E. T., "Compression of Composite Materials: A Review", Technical Report, DTRC-87/050, U. S. Navy David Taylor Research Center, Bethesda, MD, 1987.
- [13] Lee, R. J., Trevett, A. S., "Compression Strength of Aligned Carbon Fibre Reinforced Thermoplastic Laminates", Proceedings of ICCM-VI & ECCM-2, (F. L. Matthews, N. C. R. Buskell, J. M. Hodgkinson, and J. Morton, Eds.), Elsevier Applied Science Publishers LTD, London, 1987, pp. 1.278-1.287.
- [14] Leeser, D., Leach, D., "Compression Properties of Thermoplastic Matrix Composites", Proceedings of 34th International SAMPE Symposium, (G. A. Zakrzewski, D. Mazenko, S. T. Peters, and C. D. Dean, Eds.), Society for the Advancement of Material and Process Engineering, Covina, CA, 1989, pp. 1464-1473.
- [15] Scobbo, Jr. J. J., Nakajima, N., "Strength and Failure of PEEK/Graphite Fiber Composites", SAMPE Journal, Vol. 26, No. 1, 1990, pp. 45-50.
- [16] Pavier, M. J., Chester, W. T., "Compression Failure of Carbon Fibre-Reinforced Coupons Containing Central Delaminations", Composites, Vol. 21, No. 1, 1990, pp. 23-31.
- [17] Guynn, E. G., Bradley, W. L., Elber, W., "Micromechanics of Compression Failures in Open Hole Composite Laminates", Composite Materials: Fatigue and Fracture, Second Volume, ASTM STP 1012, (P. A. Lagace, ED.), American Society for Testing and Materials, Philadelphia, PA., 1989, pp.118-136.
- [18] Guynn, E. G., Bradley, W. L., "A Detailed Investigation of the Micromechanisms of Compressive Failure in Open Hole Composite Laminates", Journal of Composite Materials, Vol. 23, No. 5, 1989, pp. 479-504.
- [19] Guynn, E. G., Bradley, W. L., "Measurements of the Stress Supported by the Crush Zone in Open Hole Composite Laminates Loaded in Compression", Journal of Reinforced Plastics and Composites, Vol. 8, No. 2, 1989, pp. 133-149.
- [20] Black, N. F., Stinchcomb, W. W., "Compression Fatigue Damage in Thick, Notched Graphite/Epoxy Laminates", Long-Term Behavior of Composites, ASTM STP 813, (T. K. O'Brien, Ed.), American Society for Testing and Materials, Philadelphia, PA., 1983, pp. 95-115.
- [21] Bakis, C. E., Stinchcomb, W. W., "Response of Thick, Notched Laminates Subjected to Tension-Compression Cyclic Loads", Composite Materials: Fatigue and Fracture, ASTM STP 907, (H. T. Hahn, Ed.), American Society for Testing and Materials, Philadelphia, PA., 1986 pp. 314-334.
- [22] Bakis, C. E., Simonds, R. A., Stinchcomb, W. W., "A Test Method to Measure the Response of Composite Materials Under Reversed Cyclic Loads", Test Methods for Design Allowables for Fibrous Composites: 2nd Volume, ASTM STP 1003, (C. C. Chamis, Ed.), American Society for Testing and Materials, Philadelphia, PA., 1989, pp. 180-193.

- [23] Simonds, R. A., Bakis, C. E., Stinchcomb, W. W., "Effects of Matrix Toughness on Fatigue Response of Graphite Fiber Composite Laminates", Composite Materials: Fatigue and Fracture, Second Volume, ASTM STP 1012, (P. A. Lagace, Ed.), American Society for Testing and Materials, Philadelphia, PA., 1989, pp. 5-18.
- [24] Simonds, R. A., Stinchcomb, W. W., "Response of Notched AS4/PEEK Laminates to Tension/Compression Loading", Advances in Thermoplastic Matrix Composite Materials, ASTM STP 1044, (G. M. Newaz, Ed.), American Society for Testing and Materials, Philadelphia, PA., 1989, pp. 133-145.
- [25] Dan-Jumbo, E., Zhou, S. G., Sun, C. T., "Load-Frequency Effect on Fatigue Life of IMP6/APC-2 Thermoplastic Composite Laminates", Advances in Thermoplastic Matrix Composite Materials, ASTM STP 1044, (G. M. Newaz, Ed.), American Society for Testing and Materials, Philadelphia, PA., 1989, pp. 113-132.
- [26] Springer, G. S. (Ed.), Environmental Effects on Composite Materials, Vols. 1 and 2, Technomic Publishing Company, Lancaster, PA, 1981, 1984.
- [27] Cogswell, F. N., Hopprich, M., "Environmental Resistance of Carbon Fibre-Reinforced Polyether Etherketone", Composites, Vol. 14, No. 3, 1983, pp. 251-153.
- [28] Lhymn, C., Schultz, J. M., "Strength and Toughness of Fibre-Reinforced Thermoplastics: Effect of Temperature and Loading Rate", Composites, Vol. 18, No. 4, 1987, pp. 287-292.
- [29] Kays, A. O., Hunter, J. D., "Characterization of Some Solvent-Resistant Thermoplastic Matrix Composites", Composite Materials: Quality Assurance and Processing, ASTM STP 797, (C. E. Browning Ed.), American Society for Testing and Materials, Philadelphia, PA., 1983, pp. 119-132.
- [30] Valentin, D., Paray, F., Guetta, B., "The Hygrothermal Behavior of Glass Fibre Reinforced Pa66 Composites: A Study of the Effect of Water Absorption on their Mechanical Properties", Journal of Materials Science, Vol. 22, No. 1, 1987, pp. 46-56.
- [31] Hoa, S. V., Lin, S., Chen, J. R., "Effects of Moisture Content on the Mechanical Properties of Polyphenylene Sulfide Composite Materials", Advances in Thermoplastic Matrix Composite Materials, ASTM STP 1044, (G. M. Newaz, Ed.), American Society for Testing and Materials, Philadelphia, PA., 1989, pp. 213-230.
- [32] Wang, Q., Springer, G. S., "Moisture Absorption and Fracture Toughness of PEEK Polymer and Graphite Fiber Reinforced PEEK", Journal of Composite Materials, Vol. 23, No. 5, 1989.
- [33] Su, K. B., "Mechanisms of Interlaminar Fracture in a Thermoplastic Matrix Composite Laminate", Proceedings of the Fifth International Conference on Composite Materials, (W. C. Harrigan, Jr., J. Strife, A. K. Dhingra, Eds.), The Metallurgical Society, Inc., Warrendale, PA., 1985, pp. 995-1006.

- [34] Chang, I. Y., "Thermoplastic Matrix Continuous Filament Composites of Kevlar Aramid or Graphite Fiber", Composites Science and Technology, Vol. 24, No. 1, 1985, pp. 61-79.
- [35] Horgan, C. O., "Recent Developments Concerning Saint-Venant's Principle: An Update", Applied Mechanics Reviews, Vol. 42, No. 11, 1989, pp. 295-303.
- [36] Bogetti, T. A., Gillespie, Jr. J. W., Pipes, R. B., "Evaluation of the IITRI Compression Test Method for Stiffness and Strength Determination", Composites Science and Technology, Vol. 32, No. 1, 1988, pp. 57-76.
- [37] Jost, W., Diffusion in Solids, Liquids, and Gases, Academic Press Inc., New York, 1952, pp. 1-60.
- [38] Shen, C. H., Springer, G. S., "Moisture Absorption and Desorption of Composite Materials", Journal of Composite Materials, Vol. 10, No. 1, 1976, pp. 2-20.
- [39] Lin, C. D., "Characterization on J1 Polymer and the Effect of Moisture Uptake", Ph. D. Thesis, Department of Materials Science, College of Engineering, University of Illinois, Urbana, December, 1990.